

The tidal disruption rate in dense galactic cusps containing a supermassive binary black hole

P. B. Ivanov

Astronomy Unit, School of Mathematical Sciences, Queen Mary, University of London, UK

Astro Space Center of PN Lebedev Physical Institute, Moscow, Russia

A. G. Polnarev

Astronomy Unit, School of Mathematical Sciences, Queen Mary, University of London, UK

P. Saha

Astronomy Unit, School of Mathematical Sciences, Queen Mary, University of London, UK

28 June 2018

ABSTRACT

We consider the problem of tidal disruption of stars in the centre of a galaxy containing a supermassive binary black hole with unequal masses. We assume that over the separation distance between the black holes the gravitational potential is dominated by the more massive primary black hole. Also, we assume that the number density of stars is concentric with the primary black hole and has a power-law cusp. We show that the bulk of stars with a small angular-momentum component normal to the black-hole binary orbit can reach a small value of total angular momentum through secular evolution in the gravitational field of the binary, and hence they can be tidally disrupted by the larger black hole. This effect is analogous to the so-called Kozai effect (Kozai 1962, Lidov 1961, 1962) well known in celestial mechanics. We develop an analytical theory for the secular evolution of the stellar orbits and calculate the rate of tidal disruption. We confront our analytical theory with a simple numerical model and find very good agreement.

Our results show that for primary black-hole mass $\sim 10^6 - 10^7 M_\odot$, the black-hole mass-ratio $q > 10^{-2}$, cusp size $\sim 1\text{pc}$, the tidal disruption rate can be as large as $\sim 10^{-2} - 1 M_\odot/\text{yr}$. This is at least $10^2 - 10^4$ times larger than estimated for the case of a single supermassive black hole. The duration

of the phase of enhanced tidal disruption is determined by the dynamical-friction time scale, and it is rather short: $\sim 10^5$ yr. The dependence of the tidal disruption rate on the mass ratio, as well as on the size of the cusp, is also discussed.

Key words: black hole physics - galaxies: nuclei

1 INTRODUCTION

The problem of the tidal disruption of the stars by a supermassive black hole has attracted the attention of many researches starting from the pioneering paper of Hills 1975, who proposed that the stellar gas released from the tidally disrupted star could power quasars and AGN's. Later, it has been realized that the tidal disruption event could manifest itself as a luminosity flare in the centre of a galaxy (e.g., Gurzadian & Ozernoi 1981, Lacy et al. 1982, Rees 1988). The observational detection of these flares have recently been reported (e.g., Komossa et al. 2003 and references therein).

In order to be tidally disrupted a star must have its orbital pericentre sufficiently close to the central black hole, and accordingly, its angular momentum must be sufficiently small. Thus, the presence of the central black hole give rise to a 'loss cone' in the distribution of stars in angular-momentum space (e.g., Frank & Rees 1976), where the number of the stars is quickly exhausted due to tidal disruption, and the process of refilling the loss cone determines the rate of tidal disruption. Estimates of the rate of tidal disruption are typically based on the assumption of two-body gravitational interactions between the stars as the dominant process of angular-momentum change. Since the relaxation time associated with this process is large for realistic models of galactic centres, these estimates give rather low values of the disruption rate, of the order of 10^{-7} to $10^{-4}M_{\odot}/\text{yr}$ depending on the properties of the stellar population of the galactic centres and the mass of the black hole residing in the centre (e.g., Frank & Rees 1976, Lightman & Shapiro 1977, Shapiro & Marchant 1978, Cohn & Kulsrud 1978, Magorrian & Tremaine 1999, Syer & Ulmer 1999, Wang & Merritt 2004 and references therein). It has been pointed out by Komberg 1968 and by Polnarev and Rees 1994 that a secondary black hole of a smaller mass could intrude in the galactic centre as a result of the process of merging of two galaxies and perturb stellar trajectories, leading to non-conservation of the angular momentum and an enhancement of the tidal disruption rate (for a review of astrophysical processes occurring in galactic centres containing a supermassive black hole binary see e. g. Merritt & Milosavljevic 2004 and references therein). The purpose of

this paper is to calculate this enhanced tidal disruption rate in a simple model of interaction between the binary black hole and the stars.

We assume that the binary black hole consists of two black holes of unequal masses moving around each other in circular orbits deep inside the potential well of the primary black hole. We take into account the gravity of the central stellar cluster in the form of small corrections to the motion of stars. It has been pointed out that when the gravity is dominated by the central black hole, the number density of stars increases toward the centre according to a power law and such a distribution of the stars has been called ‘the cusp’ (Peebles 1972, Bachall & Wolf 1976, Young 1980). We use this power law distribution as the initial condition for our problem. We consider only stars with orbits within the orbit of the binary (which we will call the ‘inner problem’). We show that in this case the main process leading to the replenishment of the loss cone is a secular effect increasing the eccentricities of the stars called ‘the Kozai effect’ (Kozai 1962, Lidov 1961, 1962). The qualitative explanation of the process is very simple. Let us assume as a zeroth approximation that the stars move on Keplerian orbits in the gravitational field of the primary black hole and that gravitational interaction with the secondary black hole introduces slow secular changes to the orbital elements. Neglecting the possibility of resonance interactions and considering the evolution of the orbital parameters on a time scale much larger than the orbital periods of the star and of the binary, it is well-known that the secondary black hole can be approximated by its orbital average, which is a mass ring. Since the gravitational field of a ring is static and axially symmetric, the energy and the angular-momentum component normal to the ring plane are conserved. However, in the course of the secular evolution the total angular momentum varies with time, and it can be as small as the constant normal component. Since the number of stars whose normal component of angular momentum lies within loss-cone size is much larger than the number of stars whose total angular momentum lies within the loss cone, the number of stars which can be tidally disrupted is significantly increased by the presence of the secondary black hole.

In the next Section we formulate the model problem, which takes into account the secular evolution of the orbital elements of the stars from both the secondary black hole and the stellar cluster. The analytical solution of the secular problem is discussed in Section 3. The tidal disruption rate based on this solution is evaluated in Section 4. In Section 5 we present a numerical approach to the problem and check the validity of our analytical results. In Section 6 we use the results obtained in the previous Sections to estimate the enhanced tidal

disruption rate in astrophysical systems. This Section is written in a fairly self-contained way, so readers interested in astrophysical applications but not in the derivations of the relevant equations can go directly to this Section. Section 7 presents our conclusions and discussion.

2 FORMULATION OF THE MODEL PROBLEM

As explained in the Introduction, we would like to know how many stars are supplied on low angular-momentum orbits due to gravitational interaction with the supermassive binary black hole consisting of a primary black hole of mass M residing in the centre of a galaxy and an intruding secondary black hole with a lower mass m . The gravitational interaction of the binary black hole with stars of the stellar cluster is an extremely complicated physical process which involves dynamics of the stars in the field of two gravitating masses, effects of a slow change of orbital elements of the binary black hole due to dynamical friction and emission of gravitational radiation (e.g., Polnarev & Rees 1994, Quinlan & Hernquist 1997, Merritt & Milosavljevic 2004 and references therein) and due to interaction with an accretion disc (Ivanov, Papaloizou & Polnarev 1999), and effects caused by the gravitational potential of the stellar cluster itself. Obviously, this problem cannot be solved analytically. In order to make the problem analytically tractable while retaining the main features expected in an astrophysical situation, we consider a model where the orbital elements of a star are evolving in Newtonian gravitational field of two masses moving around each other on circular orbits. The separation distance D between two black holes remains constant with time. We also take into account the most significant effect of the gravitational field of the cluster on the stellar orbit, which is the apsidal precession of the pericentre of the orbit. The rate of this precession is calculated in Appendix A. Apart from the apsidal precession this model is the three-dimensional circular restricted three-body problem of celestial mechanics.

Since we are interested in a statistical description of the stellar orbits, we assume below that the stellar orbits are characterised by phase space distribution function $f(\vec{x}, \vec{v}, t)$. Now let us assume that at time $t = 0$ the distribution function is not perturbed by the secondary black hole and equals its unperturbed stationary value $f_0(\vec{x}, \vec{v})$. After this moment of time the gravitational influence of the secondary hole is turned on and the energies and angular momenta of the stars (defined in the frame centred at the primary black hole) start to evolve

due to perturbations induced by the secondary.* During the evolution the specific angular momentum of some stars gets smaller than a certain value l_T , corresponding to the tidal loss cone. These stars are assumed to be destroyed by the tidal forces of the primary black hole and are not considered further.

Before going to details we would like to introduce some notation, discuss some additional simplifying assumptions used later on, and specify the initial conditions for the problem.

2.1 Notation and additional simplifying assumptions

When the semi-major axis of a star is sufficiently large, close encounters of the stars with the secondary black hole are possible. These encounters change the energy and the angular momentum of the stars in a very complicated way, and the analytical treatment of these encounters is rather difficult. In this paper we do not consider these complicated issues reserving them for future work and discuss only the ‘inner problem’ concentrating on the stars with semi-major axis $a < D/2$. In this case the orbit of the star does not cross the orbit of the secondary black hole, and the theory of evolution of the star’s orbit is sufficiently simple (see below). In the following discussion we introduce dimensionless variables associated with the binary orbit: $\tilde{a} = a/D$, $\tilde{L} = L/\sqrt{GMD}$, etc. In terms of these variables the problem depends only on two parameters: the dimensionless absolute value of the angular momentum associated with the tidal loss cone $l_T = L_T/\sqrt{GMD}$ and the mass ratio $q = m/M$. Both parameters are assumed to be small, in the range $q, l_T \sim 10^{-3}$ to 10^{-1} (see Section 6).

2.2 The initial distribution function

The number of stars supplied into the tidal loss cone obviously depends on the form of the initial distribution function f_0 . In this paper we are interested in effects occurring deep inside the potential well of the primary black hole, where the number density of stars grows steeply near the centre of the stellar cluster, forming the so-called ‘cusp’ in the stellar distribution. In order to model this property of the central stellar clusters, we use the well known power-law isotropic distribution function of the stars in the phase space (e.g., Spitzer 1987, Bahcall and Wolf 1976, Lightman & Shapiro 1977)

$$f_0 = CE^p, \tag{1}$$

* We neglect the change of the energies and angular momenta due to the usual gravitational scattering of the stars. This effect seems to be very slow comparing to the effects determined by the secondary black hole.

where C is a constant, $E = GM/r - v^2/2$ is the binding energy of a star per unit mass in the field of the primary black hole of mass M , and v is the velocity of a star. According to theoretical estimates the parameter $p < 3/2$ should be rather small, and it can take two preferable values: $p = 0$ (Peebles 1972, Young 1980) and $p = 1/4$ (Bahcall and Wolf 1976). The value $p = 0$ corresponds to adiabatic growth of the cusp in an unrelaxed stellar cluster containing a growing black hole and the value $p = 1/4$ corresponds to the situation when the characteristic relaxation time is smaller than the life time of the system. Since the relaxation time is typically rather large for the systems of interest we assume below $p = 0$ for our estimates of the tidal disruption rate in astrophysical systems (see Section 6). However we present results from which the tidal disruption rate for the general case $p \neq 0$ can be easily obtained (see Section 4).

Also, let us note that after the binary black hole merging a significant part of stars may be expelled from the system and the cusp may be destroyed. In fact, the binary black hole scenario has been discussed to explain rather shallow density profiles observed in the centers of giant central galaxies situated in the centers of galaxy clusters (e.g. Faber et al, 1997). We do not consider this more complicated situation in this Paper assuming that the binary black hole is formed the first time in a particular galaxy of interest.

The number density of stars is obtained from (1) by integration over velocity space:

$$n(r) = n_a \left(\frac{r}{r_a} \right)^{-(3/2+p)}, \quad 2$$

where r_a is the radius of the cusp and n_a is the number density of stars at r_a . The constant C in equation (1) is obtained by integration of equation (1) over velocity space and comparison the result of integration with equations (2). It is related to n_a as

$$C = 2^{-5/2} \pi^{-1} \left(\frac{GM}{r_a} \right)^{-(p+3/2)} \frac{n_a}{B(3/2; p+1)}, \quad 3$$

where $B(x, y)$ is a Beta function [†] The total mass of stars inside a sphere of radius $r < r_a$ is given as

$$M_{st}(r) = 4\pi \frac{m_{st} n_a}{(3/2 - p)} r_a^3 \left(\frac{r}{r_a} \right)^{3/2-p}, \quad 4$$

where m_{st} is the star's mass and we assume hereafter that the cusp consists of stars of equal masses which are of the order of the solar mass M_\odot . The total mass of stars in the cusp must be of the order of the black hole mass M . In this paper we assume that these two masses

[†] Note the useful relations: $B(x, y) = B(y, x) = \frac{\Gamma(x)\Gamma(y)}{\Gamma(x+y)}$, where $\Gamma(x)$ is the Gamma function.

are equal: $M_{st}(r_a) = M$. This gives the normalisation condition:

$$n_a = \frac{(3/2 - p)M}{4m_{st}\pi r_a^3}. \quad 5$$

The initial distribution of the stars over the binding energies can be obtained from equation (1) by integration over the surface in the the phase space corresponding to a given value of the energy E (e.g., Spitzer 1987):

$$N_0(E) = C_E E^{p-5/2}, \quad 6$$

where $C_E = \sqrt{2}(\pi GM)^3 C$. Below, instead of the distribution of the stars over the binding energy, it will be convenient to use the distribution over the semi-major axes a :

$$N_0(a) = C_a a^{1/2-p}, \quad 7$$

where $C_a = \pi^3 2^{2-p} (GM)^{3/2+p} C$ and we use $E = GM/(2a)$.

We also need the distribution of stars in inclination angle i and angular momentum. To obtain this function let us introduce the Cartesian coordinates with origin at the primary black hole and the z axis normal to the orbital plane of the binary black hole. The inclination angle i is measured from the z axis and the z component of angular momentum, L_z , is related to its absolute as $L_z = L \cos(i)$. Assuming isotropy of the initial distribution function f_0 and using equation (7) we immediately obtain the initial distribution over the semi-major axis, inclinations and the absolute values of angular momentum, $N_0(a, i, L)$

$$N_0(a, i, L) = N_0(a) \frac{L \sin(i)}{L_a^2}, \quad 8$$

where $L_a = \sqrt{GMa}$ is the angular momentum corresponding to the circular orbit with radius a . The initial distribution function over semi-major axis, absolute values and the z -components of angular momentum follows from equation (8):

$$N_0(a, L, L_z) = N_0(a) \frac{1}{L_a^2}. \quad 9$$

3 THE SECULAR EVOLUTION

The bulk of stars supplied to the loss cone will have had small initial values of L_z (see the next Section and Fig. 6 for numerical results.) This effect is determined by a particular feature of the secular evolution of the star's orbital parameters in the gravitational field of the binary. For the Keplerian inner problem it has been pointed out by Kozai 1962 and Lidov 1961, 1962 that although the a and L_z are approximately conserved on time-scales much larger than the orbital periods of the star and the binary, while L varies with time.

Therefore, a star with small L_z initially can, in the course of secular evolution, reach a small-enough value of L to be eventually tidally disrupted by the primary black hole.

Kozai and Lidov independently derived the evolution equations for the orbital parameters using the methods of celestial mechanics. In general, these equations have a rather complicated form. However, they are simplified significantly when only the quadrupole contribution of the gravitational potential of the secondary is taken into account (e.g., Innanen, Zheng, Mikkola and Valtonen 1997, Kiseleva, Eggleton & Mikkola 1998). We use the evolution equations derived in these papers and add an extra term describing the apsidal precession caused by the gravity of the stellar cluster.

After doubly averaging over the periods of the star and the binary the relevant equations take the form

$$T_K \frac{de}{dt} = \frac{5}{2} \epsilon e \sin^2(i) \sin(2\omega), \quad (10)$$

$$T_K \frac{di}{dt} = -\frac{5}{4} e^2 \sin(2i) \sin(2\omega) / \epsilon, \quad (11)$$

$$T_K \frac{d\omega}{dt} = (2(1 - e^2) + 5 \sin^2(\omega)(e^2 - \sin^2(i))) / \epsilon - \kappa \epsilon, \quad (12)$$

$$T_K \frac{d\chi}{dt} = -(1 + e^2(5 \sin^2(\omega) - 1)) \cos(i) / \epsilon. \quad (13)$$

Here e , i , ω and χ are the eccentricity, inclination, the argument of pericentre and the longitude of ascending node, respectively, and $\epsilon = \sqrt{1 - e^2}$. T_K gives the characteristic time-scale of the Kozai effect:

$$T_K = \frac{4}{3q} \tilde{a}^{-3/2} \sqrt{\frac{D^3}{GM}}. \quad (14)$$

The last term in equation (12) describes the apsidal precession induced by the stellar cluster (see Appendix A). The parameter κ is given by

$$\kappa = K \left(\frac{T_K}{P_{orb}} \right) \left(\frac{M_{st}(a)}{M} \right) = \frac{2}{3\pi} K \left(\frac{M_{st}(a)}{m} \right), \quad (15)$$

where $P_{orb} = 2\pi\sqrt{a^3/(GM)}$ is the orbital period of the star, $M_{st}(a)$ is the total mass of the stars inside a sphere of the radius a , and the positive coefficient K is calculated in Appendix A:

$$K = 2^{3/2-p} \sqrt{\pi} \frac{\Gamma(1-p)}{\Gamma(3/2-p)}. \quad (16)$$

In our estimates below we use $K = 4\sqrt{2}$ corresponding to a cusp with the parameter $p = 0$ (see equations (1-9)). It is very important to note that the apsidal precession caused by the stellar cluster has negative sign while the sign of the apsidal precession caused by the Kozai

effect is positive. This stems from the fact that the gravitational force acting from the cluster is always directed inward, to the centre of the cluster, while the averaged gravitational force acting from the secondary black hole in the inner problem is directed outward. The opposite directions of the gravitational forces result in the opposite signs of corresponding precession rates.

The set of equations (10-13) has two integrals of motion:

$$\Lambda = \epsilon \cos(i), \quad Q = e^2(5 \sin^2(i) \sin^2(\omega) + \kappa - 2). \quad 17$$

It is obvious that the integral Λ is proportional to L_z . Using the expressions (17) we can obtain the evolutionary tracks of the dynamical system (10-13) on the plane (e, ω) :

$$\sin^2(\omega) = \frac{\epsilon^2(Q + (2 - \kappa)e^2)}{5e^2(\epsilon^2 - \Lambda^2)}. \quad 18$$

Also, we can express the inclination i and the argument of pericentre ω in terms of the eccentricity e with help of the integrals (17), substitute the result in equation (12) and obtain a single evolution equation for the eccentricity e :

$$T_K e \frac{de}{dt} = \pm \sqrt{\{((3 + \kappa + Q - 5\Lambda^2)e^2 - (3 + \kappa)e^4 - Q)(Q + (2 - \kappa)e^2)\}}. \quad 19$$

The solution of equation (19) can be expressed in terms of elliptical integrals (see below).

It can be shown that in the course of evolution of the dynamical system (10-13) the change of the eccentricity with time is cyclic (we will call these ‘Kozai cycles’) and the argument of pericentre ω can either evolve monotonically or librate around the values $\omega = \pm\pi/2$. Accordingly, solutions of equations (10-13) can be divided on two separate types of rotating (r) and librating (l) solutions. Let us discuss each types in turn. As follows from equation (10) the eccentricity e as a function of time can have its extremum only when $\omega = 0$ or $\pi/2$. In the case of the solutions of (r) type both values of $\omega = 0$ and $\omega = \pi/2$ are possible. Let us call the values of eccentricity and inclination corresponding to $\omega = 0$ ($\omega = \pi/2$) as e_0 and i_0 (e_1 and i_1). The integrals (17) can be expressed either in terms of i_0 and e_0 or i_1 and e_1 . The corresponding expressions can be equated to each other and we can obtain the inclinations i_0 and i_1 as functions of e_0 and e_1 from the resulting equations:

$$\sin^2(i_0) = \frac{1}{5e_1} \frac{(e_1^2 - e_0^2)}{(1 - e_0^2)} (2 - \kappa + (3 + \kappa)e_1^2), \quad \sin^2(i_1) = \frac{(2 - \kappa)(e_1^2 - e_0^2)}{5e_1^2}. \quad 20$$

The integrals Λ and Q can also be expressed in terms of e_0 and e_1 :

$$\Lambda^2 = \frac{(1 - e_1^2)}{5e_1^2} ((3 + \kappa)e_1^2 + (2 - \kappa)e_0^2), \quad Q = -(2 - \kappa)e_0^2. \quad 21$$

As follows from equation (20) when $\kappa < \kappa_{\text{crit}} = 2$ the maximal (minimal) value of the eccentricity is attained at $e = e_1$ ($e = e_0$) and in the opposite case of a large $\kappa > \kappa_{\text{crit}}$ the

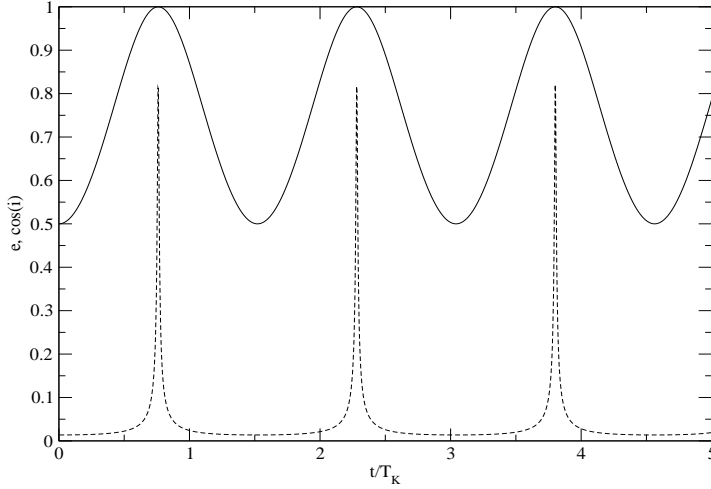


Figure 1. An example of Kozai cycles. The dependencies of eccentricity e (solid curve) and $\cos(i)$ (dashed curve) on time (in units T_K). The minimal (maximal) eccentricity is equal to 0.5 (0.9999). The minimal value of $\cos(i) \approx 0$ ($i \approx \pi/2$) corresponds to the minimal value of the eccentricity, and the maximal value of $\cos(i) \approx 0.8$ corresponds to the maximal eccentricity. The period of the cycles $P_K \approx 1.5T_K$ is in agreement with its theoretical value (see equation (24)). The case shown corresponds to the Keplerian regime ($\kappa = 0$) and the evolution of (r) type.

maximal (minimal) value of eccentricity is equal to e_0 (e_1). In the last case the minimal value of the eccentricity e_1 is always smaller than the critical value

$$e_{\text{crit}} = \sqrt{\frac{\kappa - 2}{\kappa + 3}},$$

and the maximal value e_0 is limited from above: $e_0 < \min\left(1, \sqrt{\frac{\kappa+3}{\kappa-2}}e_1\right)$. It turns out that when $\kappa > \kappa_{\text{crit}}$ only a very small number of the solutions of the (r) type would lead to a significant increase of the eccentricity, and accordingly, to a significant decrease of the total angular momentum, during the secular evolution. Therefore, these solutions are not relevant to our problem and will not be considered further (see also the end of this Section).

When $\kappa < \kappa_{\text{crit}}$ the solutions of the (r) type describe periodic changes of eccentricity and inclination, and the minimal (maximal) value of the eccentricity corresponds to the maximal (minimal) value of the inclination (see Fig. 1).

Substituting expressions (21) in equation (19) and integrating the result we find the period of the Kozai cycles:

$$P_K = \frac{2}{\sqrt{(2-\kappa)((3+\kappa)e_1^2 + (2-\kappa)e_0^2/e_1^2)}} \mathbf{K}(y)T_K, \quad 22$$

where $\mathbf{K}(k)$ is the elliptic integral of first kind and

$$y = e_1^2 \sqrt{\frac{(3+\kappa)(1-e_0^2/e_1^2)}{(2-\kappa)e_0^2 + (3+\kappa)e_1^4}}. \quad 23$$

When $\kappa = 0$ and $e_0 \ll e_1$, $e_1 \approx 1$ we have

$$P_K^0 \approx \sqrt{\frac{2}{3}} \ln \left(\sqrt{\frac{3}{5}} \frac{4}{e_0} \right) T_K, \quad (24)$$

where we use the asymptotic relation $\mathbf{K}(k \rightarrow 1) \approx \ln \frac{4}{k'}$, and $k' = \sqrt{1 - k^2}$. It is interesting to note that when $e_0 \approx e_1 \approx 1$ the period P_K^0 is finite: $P_K^0 \approx \frac{\pi T_K}{\sqrt{10}} \approx T_K$. From equation (22) it also follows that when $\kappa \rightarrow 2$ the period increases as $\propto 1/\sqrt{(2 - \kappa)}$.

Now let us discuss the librating solutions where both minima and maxima of the eccentricity are attained at $\omega = \pm\pi/2$. In this case the corresponding inclination angles and the integrals (17) can also be expressed in terms of the minimal and maximal eccentricities:

$$\sin^2(i_{\pm}) = \frac{1}{5}(2 + 3e_{\mp}^2 - \kappa(1 - e_{\mp}^2)), \quad (25)$$

and

$$\Lambda^2 = \frac{(3 + \kappa)}{5}(1 - e_-^2)(1 - e_+^2), \quad Q = (3 + \kappa)e_-^2 e_+^2, \quad (26)$$

where, by definition, e_- (e_+) is the minimal (maximal) value of the eccentricity and i_{\pm} are the inclination angles corresponding to e_{\pm} . From equation (25) it follows that when $\kappa > \kappa_{\text{crit}} = 2$ only sufficiently large eccentricities are allowed: $e_{\pm} > e_{\text{crit}} = \sqrt{\frac{\kappa - 2}{\kappa + 3}}$.

Similar to the previous case the expression for the period of the Kozai cycles is obtained by substitution of equation (26) in equation (19) and integration of the resulting differential equation. When $\kappa < \kappa_{\text{crit}}$ we have:

$$P_K = \frac{2}{e_+ \sqrt{(3 + \kappa)((3 + \kappa)e_-^2 + 2 - \kappa)}} \mathbf{K}(y) T_K, \quad (27)$$

where

$$y = \sqrt{\frac{(2 - \kappa)(1 - e_-^2/e_+^2)}{(3 + \kappa)e_-^2 + 2 - \kappa}}. \quad (28)$$

When $\kappa = 0$, $e_+ \sim 1$ and $e_- \ll 1$ we can obtain an approximate expression for P_K^0 very similar to the expression (24):

$$P_K^0 \approx \sqrt{\frac{2}{3}} \ln \left(\sqrt{\frac{3}{5}} \frac{4}{e_-} \right) T_K, \quad (29)$$

In the opposite case $\kappa > \kappa_{\text{crit}}$ we have

$$P_K = \frac{2}{(3 + \kappa)e_- \sqrt{e_+^2 - e_{\text{crit}}^2}} \mathbf{K}(y) T_K, \quad (30)$$

where

$$y = \frac{e_{\text{crit}}}{e_-} \sqrt{\frac{1 - e_-^2/e_+^2}{1 - e_{\text{crit}}^2/e_+^2}}. \quad (31)$$

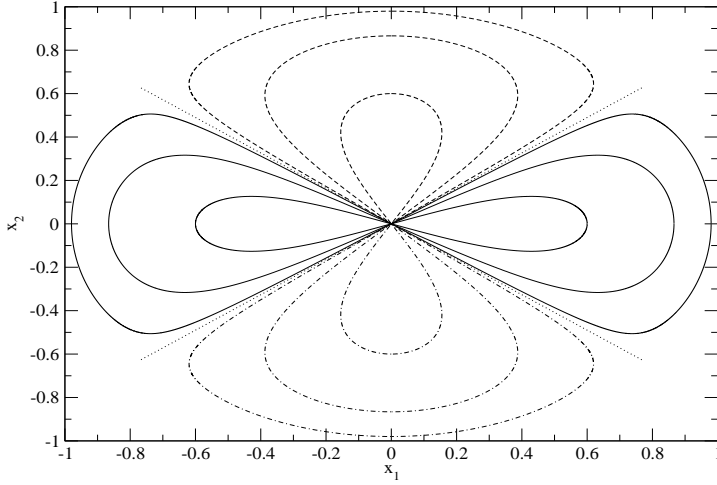


Figure 2. We show the evolutionary tracks of the dynamical system (10-12) on the plane (x_1, x_2) for the purely Keplerian case ($\kappa = 0$). The value of the integral Λ is taken to be $1 \cdot 10^{-3}$ for all curves. The solid curves represent the solutions of (r) type and the dashed and dot-dashed curves represent the solutions of (l) type. Different curves of the same type are characterised by different possible minimal values of the eccentricity, and respectively, by different maximal values of the ‘radius’ ϵ . For the curves of (r) type the minimal value of the eccentricity e_0 is attained at $\omega = 0$ and $\omega = \pi$ (when the curves cross the line $x_2 = 0$), and we present the cases $e_0 = 0.2, 0.5$ and 0.8 . The curves of (l) type have the minimal eccentricity e_- at $\omega = \pm\pi/2$ (when the curves cross the line $x_1 = 0$) and again we show the cases $e_- = 0.2, 0.5$ and 0.8 . Two dotted lines separate the regions where the librating and rotating regimes of evolution are possible (see the text).

Note that when $\kappa = \kappa_{\text{crit}}$ both expressions (27) and (29) give the same result:

$$P_K = \frac{\pi}{5e_-e_+} T_K.$$

When $e_- \rightarrow e_{\text{crit}}$ the period diverges logarithmically. Assuming that $\delta = (e_- - e_{\text{crit}})/e_{\text{crit}} \ll 1$ we find from equation (30)

$$P_K \approx \frac{2}{\sqrt{5(\kappa - 2)}} \ln \left(2 \sqrt{\frac{10}{(3 + \kappa)\delta}} \right) T_K, \quad 32$$

where we also assume that $e_+ \approx 1$ (see also equation 34). Note that the expression (32) is approximately valid only when $\delta < \delta_* = \frac{5}{(\kappa+3)}$. Also, let us point out that when both e_- and e_+ are close to unity we can obtain another approximate expression: $P_K \approx \frac{\pi T_K}{\sqrt{5(\kappa+3)}}$.

3.1 The structure of the phase space

It is convenient to represent the solutions of the different types on the plane $(x_1 = \epsilon \cos(\omega), x_2 = \epsilon \sin(\omega))$. Since $\epsilon = \sqrt{(1 - e^2)} < 1$, all solutions are situated within the unit circle. Provided that the integral Λ is fixed the curves corresponding to different solutions belong to the same two-dimensional dynamical system and do not cross each other, and we use the small $\Lambda = 1 \cdot 10^{-3}$ hereafter. We show the solutions in Figs. 2–5. Fig. 2 and Fig. 3 represent the case of $\kappa < \kappa_{\text{crit}} = 2$, specifically $\kappa = 0$ and $\kappa = 1.9$. The curves representing the

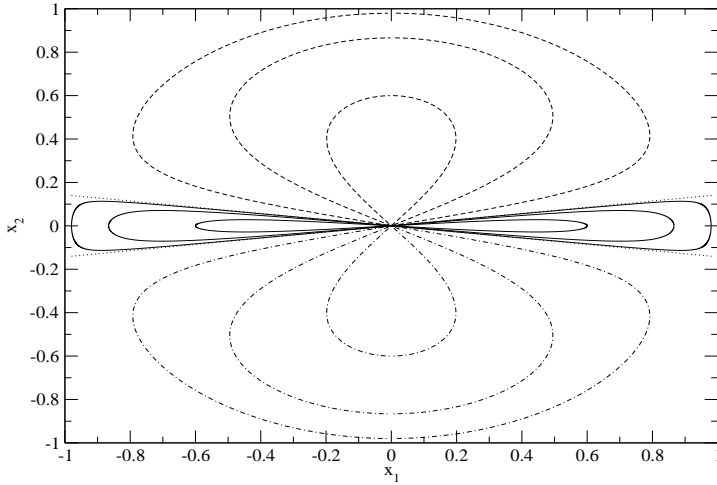


Figure 3. Similar to Fig. 2 but now $\kappa = 1.9$ is just below the critical value $\kappa_{\text{crit}} = 2$. All other parameters are the same as in Fig. 2. The shape of the curves of the different types is similar to the case $\kappa = 0$, but the lines separating the regions of different evolution have smaller inclination with respect to the axis x_1 and the librating solutions occupy more space on the plane (x_1, x_2) .

solutions of (r) type have a ‘propeller’ like shape, and the curves representing the solutions of (l) type have a ‘bulb’ like shape with ‘cones’ directed toward the origin of the coordinate system. When the eccentricity is not very large and the integral Λ is small, the curves separating the regions in the plane (x_1, x_2) , which correspond to the solutions of different types, are approximately two straight lines. Setting the value of e_0 to zero in equation (21), substituting the result in equation (18) and neglecting the value of Λ in denominator of the result we can find the inclination angles, ω_{crit} , of these lines

$$\sin(\omega_{\text{crit}}) = \pm \sqrt{\frac{2 - \kappa}{5}}. \quad 33$$

From equation (33) it follows that when $\kappa \rightarrow \kappa_{\text{crit}}$, $\omega_{\text{crit}} \rightarrow 0$.

Fig. 4 and Fig. 5 represent the case of $\kappa > \kappa_{\text{crit}}$. As we discussed above, in this case, the behaviour of the solutions of (r) type changes drastically. Contrary to the case $\kappa < \kappa_{\text{crit}}$, the solutions have minimal eccentricity at $\omega = \pm\pi/2$ and maximal eccentricity at $\omega = 0, \pi$. Also, the angle ω is rotating in the opposite negative direction compared to the previous case. The behaviour of solutions changes drastically and sharply when κ exceeds κ_{crit} . For example, in Fig. 4 we show the case of $\kappa = 2.1$ which is just above the critical value of $\kappa = 2$. One can see from this figure and Fig. 5 that only the curves of (r) type having the maximal values of eccentricity very close to the ‘critical’ value $e_{\text{crit}} = \sqrt{\frac{\kappa - 2}{\kappa + 3}}$ can have a small value of the minimal eccentricity. Since we are interested only in the solutions which can have a

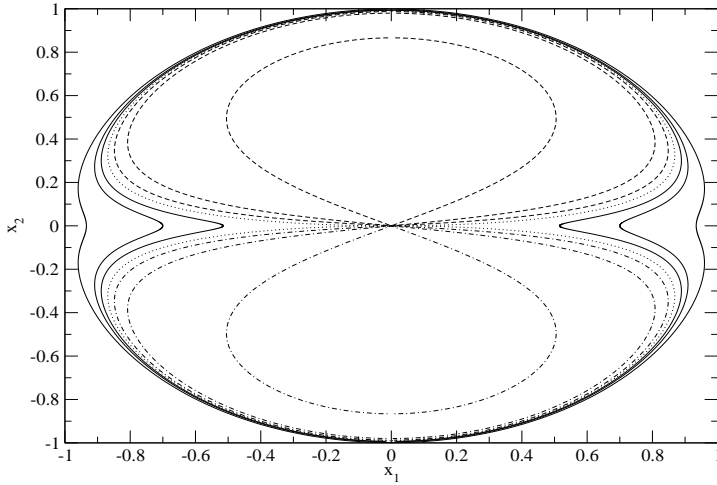


Figure 4. The case of $\kappa = 2.1 > \kappa_{\text{crit}}$ is shown. The value of Λ is the same as in the previous cases. The shape of the curves of (r) type is drastically different from the cases $\kappa = 0$ and $\kappa = 1.9$. Both rotating and librating curves have the minimal values of the eccentricity when crossing the line $x_1 = 0$ ($\omega = \pm\pi/2$). When this value is smaller (larger) than the critical value $e_{\text{crit}} \approx 0.14$ the curves belong to the family of (r) type curves ((l) type curves). As follows from the text for the curves of (r) type we define the value of eccentricity corresponding to $\omega = \pm p/2$ as e_1 . We show, respectively, the curves corresponding to $e_1 = 0.05, 0.1, 0.12$ (the solid curves) and the curves corresponding to $e_- = 0.16, 0.2$ and 0.5 (the dashed and dot dashed curves). The dotted ‘critical’ curve represents the boundary between the regions on the plane (x_1, x_2) where the motion of librating and rotating type is possible.

very large value of the eccentricity the solutions of (r) type are not interesting for us when $\kappa > 2$. On the other hand the librating solutions can produce a very large eccentricity, and therefore they are relevant to our problem even when $\kappa \gg 1$ (see Fig. 5). The solutions of both types are separated by a ‘critical’ curve which can be obtained from equations (18) and (26). For that we set $e_- = e_{\text{crit}}$ in equation (26) and substitute the result in equation (18). We have

$$\sin(\omega_{\text{crit}}) = \pm \sqrt{\frac{\kappa - 2}{5}} \frac{\epsilon}{e}. \quad 34$$

From equation (34) it follows that when κ increases the size of the regions on the plane (x_1, x_2) corresponding to the librating solutions decreases. Equation (32) also shows that the solution (34) formally has infinite period.

4 THE SUPPLY RATE OF THE STARS TO THE LOSS CONE

Now we would like to estimate the number of stars supplied to the loss cone as a function of time assuming that the initial distribution function is given by equation (9). To begin with we consider the Keplerian case, $\kappa = 0$. We also assume that the Kozai effect is solely responsible for the change of the angular momentum of the stars. As we have mentioned

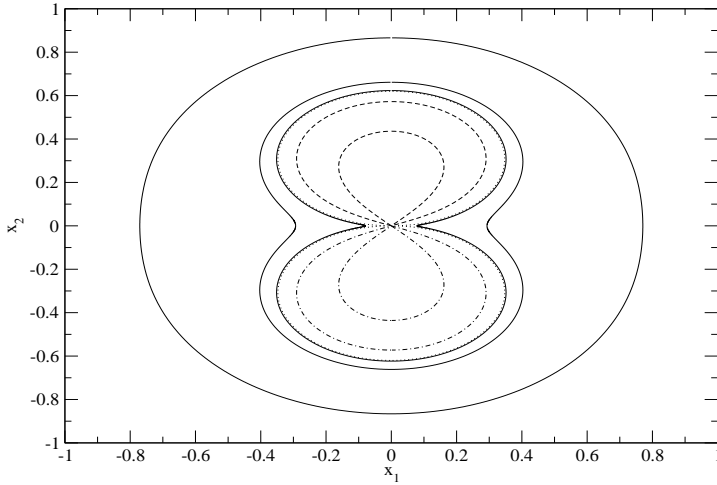


Figure 5. Similar to Fig. 4 but corresponding to $\kappa = 10$. In this case $e_{\text{crit}} \approx 0.784$ and we show the curves corresponding to $e_1 = 0.5, 0.75, 0.782$ (the solid curves) and $e_- = 0.82$ and 0.9 (the dashed and dot dashed curves). Note that apart from a small region near the origin of coordinates the dotted curve representing the boundary between the corresponding regions almost coincide with the curve corresponding to $e_1 = 0.782$.

above, the z -component of the angular momentum is approximately conserved in this case, and the number of stars per unit semi-major axis that can be supplied to the loss cone and tidally disrupted due to this effect can be estimated as the number of stars (per unit semi-major axis), $N_0^c(a)$ with L_z smaller than the size of the loss cone L_T . After integration over $L_z < L_T$ and L of the distribution (9) we obtain

$$N_0^c(a) = \int_0^{L_a} dL \int_{-L_T}^{L_T} dL_z N_0(a, L, L_z) = 2N_0(a) \frac{l_T}{\sqrt{\tilde{a}}}, \quad 35$$

where $N_0(a)$ is given by equation (7).

Let us estimate the time dependence of the number of stars supplied to the loss cone. After the moment of time $t = 0$ the number of stars with $L_z < L_T$ per unit of a , $N^c(a)$ is decreasing with time, and the rate of this decrease can be estimated as

$$\frac{dN^c(a)}{dt} = -\frac{N^c(a)}{P_K^0}, \quad 36$$

where P_K^0 is given by equations (24) and (29) for the solutions of (r) and (l) type, respectively. As follows from this equation P_K depends on the eccentricity e , and therefore, strictly speaking, in equation (36) we should divide the distribution function on P_K^0 before integration of the distribution function over the absolute value of angular momentum. However this dependence is logarithmic, say $P_K^0(e = 0.5) \approx 1.48T_K$ and $P_K^0(e = 0.9) \approx T_K$. Therefore, for simplicity, we neglect this dependence hereafter and set $P_K = T_K$ from now on. Integrating

equation (36) we obtain

$$N^c(a) = N_0^c(a)e^{-(\tilde{a}^{3/2}\tau)}, \quad 37$$

where we use equation (14), $\tau = \frac{3q}{4}\Omega_b t$, and $\Omega_b = \sqrt{\frac{GM}{D^3}}$. The number of stars $N^t(a)$ supplied to the tidal loss cone and tidally disrupted follows from equations (35) and (37):

$$N^t(a) = N_0^c(a) - N^c(a) = 2N_0(a)\frac{l_T}{\sqrt{\tilde{a}}}(1 - e^{-(\tilde{a}^{3/2}\tau)}). \quad 38$$

The total number $N^t(t)$ of stars supplied to the loss cone is obtained by integration of equation (38) over a . The integration is straightforward, with the result

$$N^t(t) = \int_0^{a_{\max}} da N^t(a) = \frac{2l_T}{(1-p)} C_a D^{(3/2-p)} \tilde{a}_{\max}^{(1-p)} \left(1 - \frac{2(1-p)}{3} x^{-2/3(1-p)} \gamma(2/3(1-p); x)\right), \quad 39$$

where $x = \tilde{a}_{\max}^{3/2}\tau$, and $\gamma(\beta, x)$ is the incomplete gamma function, a_{\max} is the upper limit of integration and we set the lower limit to zero. As we have discussed above we assume that $\tilde{a}_{\max} \approx 1/2$ for the inner problem[‡]. Note, that to obtain equation (39) we use the explicit form of the initial distribution function over a given by equation (7).

It is very important to point out that $N^t(t)$ depends linearly on the small parameter l_T . The fact that the dependence is linear leads to a significant increase of tidally disrupted stars in the presence of the secondary black hole (see Section 6). In contrast to this result the usual estimate of the tidal disruption rate due to two-body star-star gravitational scattering, in the so-called ‘full’ loss cone approximation (e.g., Hills 1975, Frank & Rees 1976) leads to a quadratic dependence. In the last case, the tidal disruption rate is proportional to the probability to find a star inside a circle in the angular momentum space of radius L_T , which is proportional to the area of this circle πL_T^2 . As we have mentioned above, in the presence of the secondary black hole only the z component of angular momentum is conserved, while total angular momentum varies due to the Kozai effect and can be evolved to a very small value $L < L_T$. Hence, in our case the tidal disruption rate is proportional to probability of finding a star with $L_z < L_T$. Note that in this respect our problem is similar to the problem of tidal disruption in a non-spherical galaxy where there is a tidal loss ‘wedge’ instead of the tidal loss cone, and the tidal disruption rate is enhanced (e.g., Magorrian & Tremaine 1999).

For comparison of our theory with results of numerical computations it is more convenient to use the probability $Pr(t)$ for a star to find itself in the tidal loss cone. This can be obtained

[‡] Note, that the quadrupole approximation used in our analysis is, strictly speaking, invalid in the case of rather large $\tilde{a}_{\max} = 1/2$. However, we assume that the estimates based on this assumption are correct in order of magnitude.

dividing the expression (39) by the total initial number of stars with semi-major axes smaller than a_{\max} , N_{tot} . This number directly follows from equation (7)

$$N_{\text{tot}} = \frac{C_a}{(3/2 - p)} a_{\max}^{3/2-p}. \quad (40)$$

Using equations (36) and (40) we obtain

$$Pr(t) = \frac{(3-2p)}{(1-p)} \frac{l_T}{\sqrt{\tilde{a}_{\max}}} \left(1 - \frac{2(1-p)}{3} x^{-2/3(1-p)} \gamma(2/3(1-p); x)\right). \quad (41)$$

The estimates shown above are approximately valid only for sufficiently large values of the loss cone l_T . The results of numerical calculations (see the next Section) show that when l_T is sufficiently small equations (39) and (41) significantly underestimate the number of stars supplied to the loss cone. To explain this effect let us consider the evolution of angular momentum on time scales of the order of the binary orbital period $P_b = 2\pi\Omega_b^{-1}$, which is much smaller than the Kozai time scale T_K . It turns out that the angular momentum oscillates on the time scale $\sim P_b$ around an averaged value determined by the secular evolution on the time scale $\sim T_K$. The largest amplitude of these oscillations is reached near the maximal value of the averaged eccentricity e_{\max} provided by the Kozai effect, and, respectively, near the minimal value of the angular momentum (see Appendix 1). The maximal amplitude, ΔL is estimated in Appendix B as

$$\Delta l = \frac{15}{8} \sqrt{\frac{3}{5}} q \tilde{a}^2, \quad (42)$$

where $\Delta l = \Delta L / \sqrt{GMD}$, and we take into account the fact that when $\kappa = 0$ both rotating and librating solutions have $\cos(i_{\min}) \approx \sqrt{\frac{3}{5}}$ (see equations (20) and (29)). It follows from equation (42) that when the size of the loss cone is very small, $l_T \ll q$, the maximal value of L_z of stars that can be supplied to the loss cone is of the order of $\Delta l \gg l_T$. Accordingly, the number of stars supplied in the loss cone is determined by Δl :

$$N_0^c(a) = \int_0^{L_a} dL \int_{-\Delta L}^{\Delta L} dL_z N_0(a, L, L_z) = 2N_0(a) \frac{\Delta l}{\sqrt{\tilde{a}}} = \frac{15}{4} \sqrt{\frac{3}{5}} q C_a D^{1/2-p} \tilde{a}^{2-p}, \quad (43)$$

where we use equations (7), (9) and (42).

Similar to the case discussed above the number of stars per unit interval of a with $L_z < \Delta L$, $N^c(a)$ decreases with time. It is important to note that in the case of the small tidal loss cone the probability of a star with $L_z < \Delta L$ to obtain the absolute value of angular momentum smaller than L_T during one Kozai cycle is of the order of $L_T / \Delta L \ll 1$. Accordingly, the rate of decrease of the number of stars with $L_z < \Delta L$ (per unit of semi-major axis) can be estimated as

$$\frac{dN^c(a)}{dt} \approx - \left(\frac{L_T}{\Delta L} \right) \frac{N^c(a)}{T_K} = - \frac{2l_T}{\sqrt{15\tilde{a}}} N^c(a) \Omega_b. \quad (44)$$

Integrating equation (44) we obtain

$$N^c(a) = N_0^c(a)e^{-(\tau_1/\sqrt{\tilde{a}})}, \quad (45)$$

where $\tau_1 = \frac{2l_T}{\sqrt{15}}\Omega_b t$, and the number of stars supplied to the loss cone is

$$N^t(a) = N_0^c(a) - N^a(a) = N_0^c(a)(1 - e^{-(\tau_1/\sqrt{\tilde{a}})}). \quad (46)$$

The total number $N^t(t)$ of stars supplied to the loss cone is obtained again by integration of equation (46) over a with the result

$$N^t = \int_0^{a_{\max}} da N^t(a) = \frac{15}{4} \sqrt{\frac{3}{5}} q \frac{\tilde{a}_{\max}^{3-p}}{(3-p)} C_a D^{3/2-p} (1 - I), \quad (47)$$

where

$$I = \frac{3-p}{\tilde{a}_{\max}^{3-p}} \int_0^{\tilde{a}_{\max}} d\tilde{a} \tilde{a}^{2-p} e^{-(\tau_1/\sqrt{\tilde{a}})}, \quad (48)$$

and the probability for a star to find itself in the tidal loss cone, $Pr_1 = N^t/N_{\text{tot}}$ is

$$Pr_1 = \frac{15}{8} \sqrt{\frac{3}{5}} \frac{(3-2p)}{(3-p)} q \tilde{a}_{\max}^{3/2} (1 - I). \quad (49)$$

The integral (48) can be estimated in terms of elementary functions in two limiting cases.

Assuming that the argument in the exponent in (48) is sufficiently small, $\tau_1 < \sqrt{\tilde{a}_{\max}}$, we can set $\tilde{a} = \tilde{a}_{\max}$ in the exponent. In this case we have

$$I \approx e^{-(\tau_1/\sqrt{\tilde{a}_{\max}})}, \quad (50)$$

and in the opposite case of a large time $\tau_1 > \sqrt{\tilde{a}_{\max}}$, the integral is estimated to be

$$I \approx 2(3-p) \frac{\sqrt{\tilde{a}_{\max}}}{\tau_1} e^{-(\tau_1/\sqrt{\tilde{a}_{\max}})}. \quad (51)$$

Taking into account the effect of additional oscillations of the angular momentum on the time scale of the binary orbital period significantly improves agreement between our theory and numerical calculations (see the next Section).

4.1 The case $\kappa \neq 0$

When $\kappa \neq 0$ the estimates of the number of stars supplied to the tidal loss cone must be modified. However, as we discussed in the previous Section, when $\kappa < \kappa_{\text{crit}} = 2$ the secular evolution of the orbital elements of the stars is very similar to the case $\kappa = 0$, and therefore we do not discuss this case later on, assuming that our expressions (39), (41) and (47), (49) give a correct order of magnitude estimate. When $\kappa > 2$ only the librating solutions of the secular equations (10–13) could produce a significant change of the eccentricity. Therefore, only the stars having orbital elements corresponding to the secular evolution of (I) type can be tidally disrupted provided that the L_z of these stars is sufficiently small. As follows from

equation (34) the boundary between the solutions of (l) and (r) types can be defined as a closed ‘critical’ curve in the plane (ϵ, ω) , and therefore, in order to estimate the number of stars going to the loss cone, we should introduce the initial distribution function of stars over the semi-major axes, the quantities $\epsilon = \sqrt{1 - e^2}$, L_z and the argument of pericentre ω , $N_0(a, \epsilon, L_z, \omega)$. Taking into account that the distribution of stars is assumed to be the uniform over ω and that $\epsilon = L/L_a$, the distribution function $N_0(a, \epsilon, L_z, \omega)$ can be easily obtained from equation (9):

$$N_0(a, \epsilon, L_z, \omega) = \frac{N_0(a)}{2\pi L_a}. \quad 52$$

We find the number of stars (per unit semi-major axis) that can be supplied to the tidal loss cone, $N_{0,\kappa}^c$, integrating the distribution function (52) over the surface under the ‘critical’ curve (34), and also integrating over L_z :

$$N_{0,\kappa}^c(a) = \int_{-L_*}^{L_*} dL_z \iint_S dS N_0(a, \epsilon, L_z, \omega) = \frac{4}{\pi} \arcsin \left(\sqrt{\frac{5}{\kappa + 3}} \right) \frac{l_*}{\sqrt{a}} N_0(a), \quad 53$$

where $\iint_S dS (\dots)$ implies integration over the surface in the plane (ϵ, ω) within the ‘critical’ curve (34), and l_* is the absolute value (in units of \sqrt{GMD}) of the z component of angular momentum of the stars supplied to the loss cone. As we discussed above when $l_T \gg q$ we have $l_* \approx l_T$ and in the opposite limit $l_* \approx \Delta l$ where Δl is given by equation (42).

As follows from equations (30) and (32) the period of Kozai cycles P_K depends on κ , and on the maximal and minimal eccentricities e_{\pm} . Also, the period is formally infinite for the solution corresponding to the critical curve (34). We are interested in the case of a high maximal eccentricity $e_{\max} \approx 1$ and the minimal eccentricity close to the critical eccentricity e_{crit} . Therefore, we use the approximate value of P_K given by equation (32). Note that this value formally depends on the eccentricity e_- through the quantity $\delta = (e_- - e_{\text{crit}})/e_{\text{crit}}$. However, since δ enters the expression (32) only in the logarithmic factor we expect that the use of a definite value of δ is irrelevant for our order of magnitude estimates, and for definiteness we set its value to the ‘typical’ value $\delta_* = \sqrt{\frac{5}{\kappa + 3}}$. We have:

$$P_K \approx \frac{2 \ln(2\sqrt{2})}{\sqrt{5(\kappa - 2)}} T_K \approx \frac{2}{\sqrt{5(\kappa - 2)}} T_K. \quad 54$$

It is very important to note that both the number of stars supplied to the loss cone $N_{0,\kappa}^c(a)$ and the period of Kozai cycles P_K^κ are proportional to the same quantities corresponding to the case $\kappa = 0$: $P_K = C_1 T_K$, and $N_{0,\kappa}^c(a) = C_2 N_0^c(a)$, where C_1 is determined by equation

(54), and C_2 follows from equations (35), (43) and (53):

$$C_2 = \frac{4}{\pi} \arcsin \left(\sqrt{\frac{5}{\kappa + 3}} \right). \quad 55$$

That means that the results obtained above for the case $\kappa = 0$ can be used when calculating the number of stars supplied to the loss cone for a non-zero value of κ . We should only multiply the expressions (39), (40) and (47), (49) by the correction factor C_2 and also make an appropriate change of the time variables entering these expression with the help of equation (54). When $l_T \gg q$ we obtain from equations (41), (54) and (55) the expression for the probability for a star to find itself in the loss cone, $Pr_\kappa(t)$:

$$Pr_\kappa(t) = C_2 Pr(t) = \frac{4(3-2p)}{\pi(1-p)} \arcsin \left(\sqrt{\frac{5}{\kappa + 3}} \right) \frac{l_T}{\sqrt{\tilde{a}_{\max}}} \left(1 - \frac{2(1-p)}{3x^{2/3(1-p)}} \gamma\left(\frac{2}{3}(1-p); x_\kappa\right) \right), \quad 56$$

where

$$x_\kappa = x/C_1 = \frac{3}{8} \sqrt{5(\kappa - 2)} \tilde{a}_{\max}^{3/2} q \Omega_b t. \quad 57$$

In the opposite case $l_T \ll q$ we use equations (49), (54) and (55)

$$Pr_{1,\kappa}(t) = C_2 Pr_1(t) = \frac{15(3-2p)}{2\pi(3-p)} \arcsin \left(\sqrt{\frac{5}{\kappa + 3}} \right) q \tilde{a}_{\max}^{3/2} (1 - I(\tau_{1,\kappa})), \quad 58$$

where

$$\tau_{1,\kappa} = \sqrt{\frac{3}{5}} \tau_1 / C_1 = \sqrt{\frac{\kappa - 2}{5}} l_T \Omega_b t, \quad 59$$

and the quantity I is given by equation (48). Note that we discard the factor $\sqrt{\frac{3}{5}}$ in equation (42) and accordingly in equations (44)-(49) to obtain equations (58) and (59). This accounts for the coefficient $\sqrt{\frac{3}{5}}$ in equation (59). As follows from equation (25), for the eccentricities $e_- \approx e_{\text{crit}}$, $\sin(i_{\min}) \approx 0$ and accordingly $\cos(i_{\min}) \approx 1$. This is different from the case of $\kappa = 0$ where $\cos(i_{\min}) \approx \sqrt{\frac{3}{5}}$.

4.2 Characteristic rates and time scales

In general the expressions for the number of stars supplied to the loss cone given by equations (39), (41), (47), (49) and (56), (58), are rather complicated functions of time. They also involve many parameters determined by the properties of a particular stellar cluster and a binary black hole. These complicated expressions are rather difficult to use. Also, in fact, they are not needed for rough estimates of the tidal disruptions rate in the presence of the black hole binary. Here, we would like to obtain much simpler order of magnitude expressions which will be used in Section 6 for these estimates. For simplicity, we also assume that the

mass of the stellar cluster is much larger than the mass of the secondary black hole, and accordingly, formally consider the case of high values of $\kappa \gg 1$.

In order to obtain the total probabilities for a star to be tidally disrupted let us consider the limit $t \rightarrow \infty$ in equations (56) and (58). In this limit, the second terms in the brackets in (56) and (58) are equal to zero and we have

$$Pr_{\text{tot}} = Pr_{\kappa}(t \rightarrow \infty) \approx \frac{4\sqrt{5}}{\pi} \frac{(3-2p)}{(1-p)} \frac{l_T}{\sqrt{\tilde{a}_{\text{max}}\kappa}} \quad (60)$$

from equation (56), and

$$Pr_{\text{tot},1} = Pr_{1,\kappa}(t \rightarrow \infty) \approx \frac{15\sqrt{5}}{2\pi} \frac{(3-2p)}{(3-p)} \frac{\tilde{a}_{\text{max}}^{3/2}}{\sqrt{\kappa}} q, \quad (61)$$

from equation (58). The characteristic tidal disruption rate $\dot{P}r$ per star can be obtained from equations (56) and (58) by differentiation these equations over the time and setting $t = 0$ in the resulting expressions. We have

$$\dot{P}r = \dot{P}r_{\kappa}(t = 0) = \dot{P}r_{1,\kappa}(t = 0) = \frac{15}{\pi} \frac{(3-2p)}{(5-2p)} \tilde{a}_{\text{max}} q l_T \Omega_b^{-1}. \quad (62)$$

Let us note that the quantity $\dot{P}r$ does not depend on κ . The characteristic time scales associated with the process of tidal disruption, T_* and $T_{*,1}$ can be obtained from equations (60), (61) and (62). When $l_T \gg q$ we have

$$T_* = Pr_{\text{tot}}/\dot{P}r = \frac{4}{3\sqrt{5}} \frac{(5-2p)}{(1-p)} \frac{\tilde{a}_{\text{max}}^{-3/2}}{\sqrt{\kappa}} (q\Omega_b)^{-1}, \quad (63)$$

and in the opposite case $l_T \ll q$ we have

$$T_{*,1} = Pr_{\text{tot},1}/\dot{P}r = \frac{\sqrt{5}}{2} \frac{(5-2p)}{(3-p)} \frac{\tilde{a}_{\text{max}}^{1/2}}{\sqrt{\kappa}} (l_T\Omega_b)^{-1}. \quad (64)$$

As we discussed in Section 2, the typical values of the parameter p are close to zero. Therefore, we can further simplify expressions (60)-(63) setting $p = 0$ and $\tilde{a}_{\text{max}} = 1/2$ and expressing κ in terms of the ratio of the total mass of the stars to the mass of the secondary, M_{st}/m with help of equations (15) and (16):

$$\kappa = \frac{8\sqrt{2}}{3\pi} \frac{M_{st}(a_{\text{max}})}{m} = \frac{4}{3\pi} \frac{M_{st}(D)}{m} \approx 0.4 \frac{M_{st}(D)}{m}, \quad (65)$$

where we take into account that when $p = 0$, $M_{st}(a) \propto a^{3/2}$ (see equation 4).

We have

$$\dot{P}r = \frac{9}{2\pi} q l_T \Omega_b^{-1} \approx 1.4 q l_T \Omega_b \quad (66)$$

from equation (62),

$$Pr_{\text{tot}} = 6\sqrt{\frac{30}{\pi}} \sqrt{\frac{m}{M_{st}}} l_T \approx 18.5 \sqrt{\frac{m}{M_{st}}} l_T, \quad (67)$$

$$T_* = 4\sqrt{\frac{10\pi}{3}}\sqrt{\frac{m}{M_{st}}}(q\Omega_b)^{-1} \approx 13\sqrt{\frac{m}{M_{st}}}(q\Omega_b)^{-1}, \quad 68$$

from equations (60), (63), and

$$Pr_{tot,1} = \frac{15}{8}\sqrt{\frac{15}{2\pi}}\sqrt{\frac{m}{M_{st}}}q \approx 2.9\sqrt{\frac{m}{M_{st}}}q, \quad 69$$

$$T_{*,1} = \frac{5}{4}\sqrt{\frac{5\pi}{6}}\sqrt{\frac{m}{M_{st}}}(l_T\Omega_b)^{-1} \approx 2\sqrt{\frac{m}{M_{st}}}(l_T\Omega_b)^{-1}, \quad 70$$

from equations (61) and (64). Equations (66–70) are used in Section 6 for estimates of the tidal disruption rate in astrophysical systems. Although equations (66–70) have been formally obtained in the limit $\kappa \gg 1$ they can also be used for order of magnitude estimates even when $\kappa \sim 1$.

5 NUMERICAL CALCULATIONS

Now we would like to discuss our numerical calculations of the supply rate and compare them to the analytical theory developed above. In our numerical work we neglect the influence of the stellar cluster on the orbits of the stars, and accordingly set $\kappa = 0$ reserving the general case $\kappa \neq 0$ for a future investigation. We consider evolution of a large number of particles in the Keplerian gravitational field of the binary for a sufficiently long time, assuming that all particles which have the absolute value of angular momentum smaller than a certain value l_T are ‘tidally disrupted’ by the primary black hole. The ‘tidally disrupted’ particles are removed from the calculations. The initial orbital elements of the particles are randomly distributed according to the distribution (8) with $p = 0$. The initial semi-major axes of the particles are in the range ($0.1 < \tilde{a} < 0.5$). The calculations depend on two dimensionless parameters: the mass ratio q and the dimensionless size of the loss cone l_T , and we consider the cases $q = 1 \cdot 10^{-2}, 3 \cdot 10^{-2}, 1 \cdot 10^{-1}$ and $l_T = 1 \cdot 10^{-3}, 3 \cdot 10^{-3}, 1 \cdot 10^{-2}, 3 \cdot 10^{-2}, 1 \cdot 10^{-1}$, respectively. For given values of q and l_T we evolve approximately $10^4 - 5 \cdot 10^4$ particles with different orbital parameters during the time $t < t_{\max} = \frac{30}{q}\Omega_b^{-1}$.

In Fig. 6 we show the distribution of the ‘tidally disrupted stars’ over the initial values of the z component of angular momentum, for the case $q = 0.1$ and different values of l_T . One can see that this distribution is strongly peaked at $L_z = 0$. This strongly suggests that the effects of the Kozai type are responsible for the supply of the particles on low angular momentum orbits in our problem. The spread of the distribution decreases with decrease of l_T . However, even for the smallest value of $l_T = 1 \cdot 10^{-3}$ the spread is of the order of

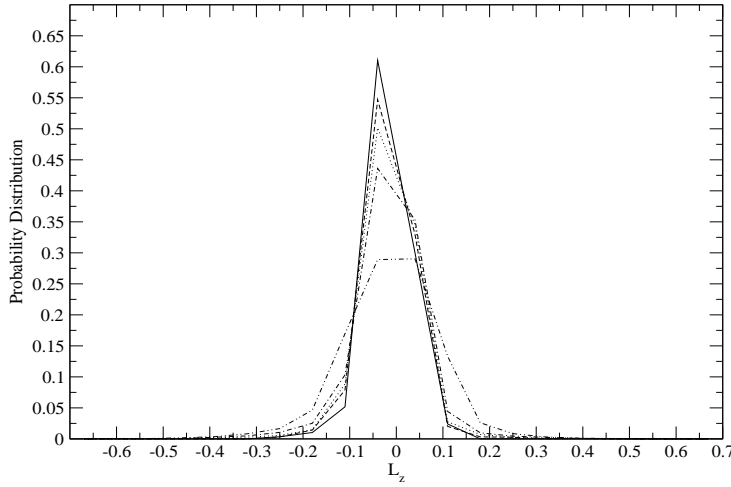


Figure 6. The distribution of the ‘tidally disrupted particles’ over the initial values of the z component of angular momentum (in unit \sqrt{GMa}). The case $q = 1$ is shown. The solid, dashed, dotted, dot-dashed and dot-dot-dashed curves correspond to $l_T = 1 \cdot 10^{-3}$, $3 \cdot 10^{-3}$, $1 \cdot 10^{-2}$, $3 \cdot 10^{-2}$, $1 \cdot 10^{-1}$, respectively.

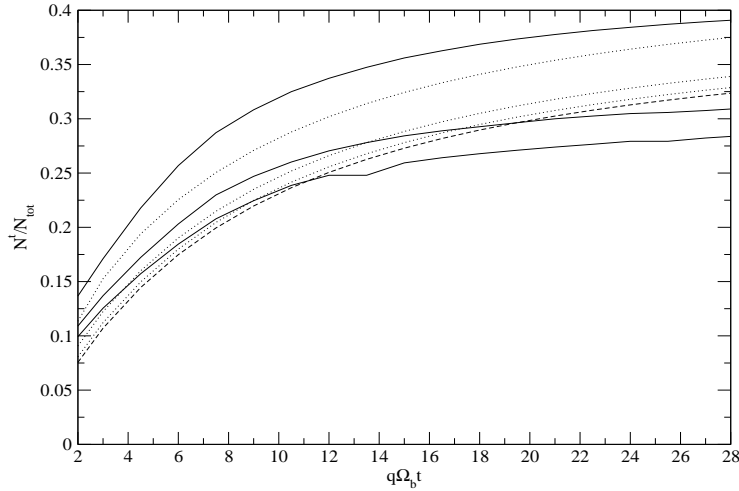


Figure 7. The dependence of the number of stars supplied to the loss cone (in units of the total number of stars participating in the calculation) as a function of time (in units of $q^{-1}\Omega_b^{-1}$). The size of the loss cone is large: $l_T = 0.1$. The three solid curves correspond to $q = 1 \cdot 10^{-2}$, $3 \cdot 10^{-2}$, $1 \cdot 10^{-1}$, with smaller values of ordinates (at a given moment of time) corresponding to smaller values of q . The dashed curve represents the theoretical solution (41) which does not depend on q in these time units. The dotted curves represent the sum of the solutions (41) and (49). The smaller ordinates correspond again to the smaller values of q .

$\sim 0.1 \gg l_T$. This can be explained by the additional oscillations of the angular momentum due to gravitational influence of the secondary on the time scale of order of the binary orbital period, see equation (42) and Appendix B. The distributions corresponding to the smaller values of q have a similar character and are not shown here.

In Fig. 7 we show the numerical and theoretical values of probability for a star to find

itself in the loss cone as a function of time, for a large value of the size of the tidal loss cone. As follows from the theoretical solution (41), in the simplest approximation this probability depends on the mass ratio only in the combination $q\Omega_b t$. That means that when the size of the loss cone is large and fixed, the numerical values of the probability (solid curves) should be approximately the same being plotted as functions of the time variable $q\Omega_b t$. In order to check this theoretical prediction we show the results of the numerical calculations for a very large and somewhat unrealistic size of the loss cone $l_T = 0.1$. As follows from Fig. 7 this theoretical prediction is qualitatively confirmed in the calculations, although the difference between the numerical curve corresponding to $q = 0.1$ and $q = 3 \cdot 10^{-2}$ and $1 \cdot 10^{-2}$ is rather large, of the order of ~ 25 – 30 per cent. The agreement between the theory and numerical calculations can be improved significantly if we take into account the effect of oscillation of the angular momentum on the orbital time scale and add the probability Pr_1 corresponding to this effect (see equation 49) to the probability Pr determined by the Kozai effect (equation 25).[§] The curves representing the sum $Pr_{\text{tot}} = Pr + Pr_1$ are shown as the dotted curves in Fig. 7. The curves corresponding to the mass ratios $q = 1 \cdot 10^{-2}$ and $3 \cdot 10^{-2}$ are close to the curve representing $Pr(t)$. The difference between these curves and those which represent the numerical calculations is about ~ 10 – 15 per cent. The dotted curve corresponding to $q = 0.1$ is rather close to the numerical curve with the difference of the order of ~ 6 – 10 per cent. Therefore, when the size of the loss cone is large the use of the total probability Pr_{tot} instead of Pr improves the agreement between the theory and the numerical calculations.

In Figs. 8, 9 and 10 we show the dependencies of numerical and theoretical values of the probability for the particle to be supplied to the loss cone calculated for realistic values of the loss cone $l_T = 1 \cdot 10^{-3}$ and $l_T = 3 \cdot 10^{-3}$. The mass ratio is equal to 0.1, $3 \cdot 10^{-2}$, $1 \cdot 10^{-2}$ in Fig. 8, Fig. 9 and Fig 10, respectively. The general behaviour of the curves is similar in all cases. The curves corresponding to $l_T = 3 \cdot 10^{-2}$ are better described by the theoretical curve representing the total probability $Pr_{\text{tot}}(t)$. On the other hand the curves corresponding to a very small $l_T = 1 \cdot 10^{-2}$ are much better described by the curve representing the probability $Pr_1(t)$. Note, that the agreement between the theoretical and numerical values is very good in the case $q = 0.1$, and the theoretical and numerical curves almost coincide in this case. The disagreement grows with decrease of the mass ratio q , and in the case $q = 1 \cdot 10^{-2}$ is

[§] Note that we use the approximate values of the integral I in the expression for the probability Pr_1 . When the time variable $\tau_1 < 6$ we use the expression (33), and when $\tau_1 > 6$ we use the expression (34). When $\tau_1 = 6$ both expressions are equal.

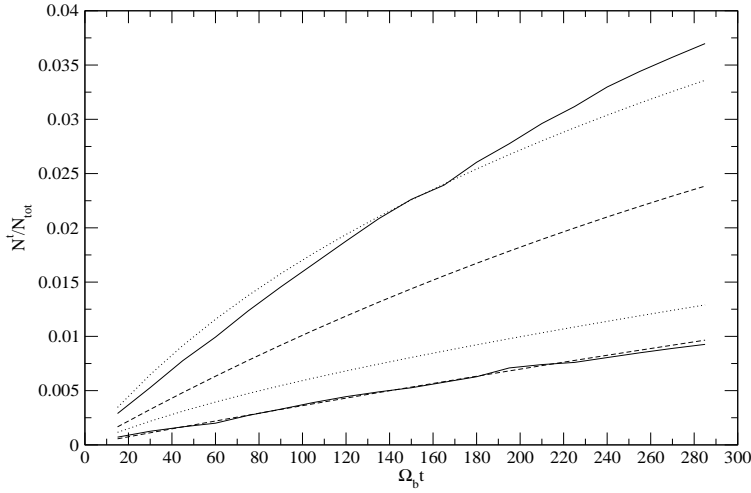


Figure 8. The dependence of the number of stars supplied to the loss cone (in units of the total number of stars) as a function of time (in units Ω_b^{-1}) for $q = 0.1$ and the small values of the loss cone. The upper solid curve corresponds to $l_T = 3 \cdot 10^{-3}$ and the lower solid curve corresponds to $l_T = 1 \cdot 10^{-3}$. The dashed and dotted curves represent the theoretical values of $Pr_1(t)$ and $Pr_{\text{tot}}(t)$, respectively. The upper (lower) dashed and dotted curves correspond to $l_T = 3 \cdot 10^{-3}$ ($l_T = 1 \cdot 10^{-3}$).

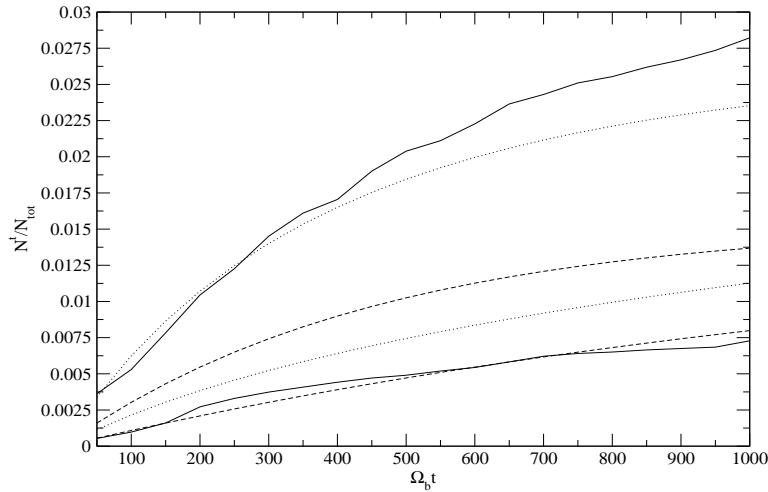


Figure 9. Same as Fig. 4 but calculated for $q = 3 \cdot 10^{-2}$.

about ~ 10 per cent. Thus, in the case of a very low size of the loss cone the probability for the particle to be supplied to the loss cone is mainly determined by the effect of oscillations of the angular momentum on the binary orbital time scale, and respectively, by equation (49). In fact, the numerical results demonstrate that for a rough estimate in the case of a large ratio l_T/q we can use the expression for the probability determined by the Kozai effect (equation 41) while in the opposite case of the small ratio l_T/q the expression (49)

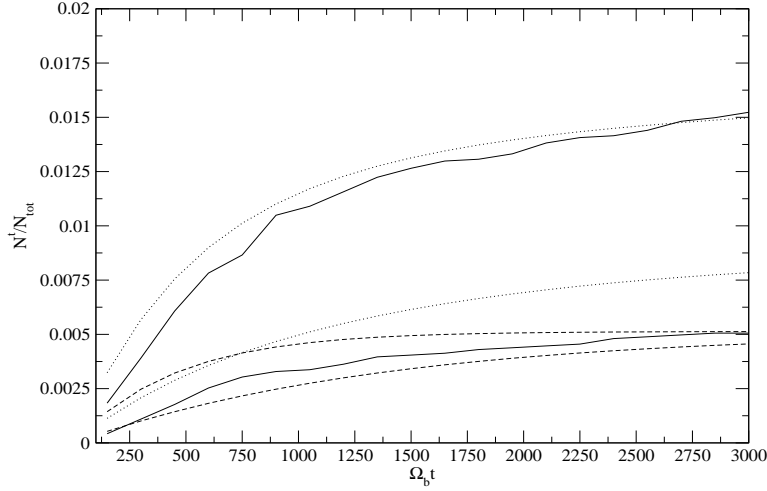


Figure 10. Same as Fig. 4 and Fig. 5 but calculated for $q = 1 \cdot 10^{-2}$.

determined by the effect of the oscillations of the angular momentum. As we have discussed above, this conclusion is well motivated from theoretical point of view.

6 ASTROPHYSICAL APPLICATIONS

6.1 The size of the tidal loss cone

We do not concentrate in this paper on complicated issues related to the problem of tidal disruption of a star, and use the simplest criterion of the tidal disruption event assuming that all stars having pericentres R_p smaller than the so-called ‘tidal’ radius R_T are tidally disrupted:

$$R_p < R_T = \left(\frac{M}{m_{st}} \right)^{1/3} R_{st} \approx 1.5 \cdot 10^{13} M_7^{1/3} \text{cm}, \quad 71$$

where we assume that all stars have solar masses and radii $R_{st} \approx 7 \cdot 10^{10} \text{cm}$ and $M_7 = M/10^7 M_\odot$. A simple estimate (Hills, 1975, Beloborodov et al 1992) shows that when the mass of the central black hole is larger than the ‘critical mass’ $M \sim 1 \cdot 10^8 M_\odot$ the stars are swallowed by the black hole without disruption, and therefore the range of the black hole masses interesting for the tidal problem is limited from above: $M < 1 \cdot 10^8 M_\odot$.¶ On the other hand, at the present time there is no observational evidences of black holes masses within

¶ Note, however that a rotating black hole of mass $\sim 10^9 M_\odot$ can actually disrupt the stars due to effects of General Relativity (Beloborodov et al 1992, Ivanov, Chernyakova & Novikov, 2003). The tidal disruption rate is suppressed in this case by a geometrical factor, and we neglect this effect later on.

the intermediate mass range $M < 10^5 M_\odot$ (e.g., Kormendy & Gebhardt 2001 and references therein), and therefore we assume that our parameter q cannot be smaller than $\sim 10^{-3}$. The specific angular momentum L_T associated with R_T is obtained from the standard Keplerian relation $L_T = \sqrt{2GM R_T}$. Following from the previous Sections, in our calculations we use the dimensionless angular momentum variable $l_T = L_T/\sqrt{GM D}$, where D is the separation distance between the two black holes. The numerical value of l_T can easily be obtained from equation (71):

$$l_T \approx 3 \cdot 10^{-3} M_7^{1/6} (\tilde{D} r_1)^{-1/2}, \quad 72$$

where $\tilde{D} = D/r_a$ and $r_1 = r_a/1\text{pc}$. We see a rather weak dependence of the numerical value of l_T on the parameters, especially on the mass of the central black hole.

6.2 The dynamical friction

When the secondary black hole enters the cusp it interacts with the stars in the cusp and continues to spiral down to the centre of mass due to the effect of dynamical friction. As a result the separation distance between the primary and the secondary black holes is a decreasing function of time $D(t)$. To estimate the characteristic time scale associated with this process we have to specify the distribution function of the stars in the cusp as well as the orbital parameters of the binary. As we have mentioned above we assume that the binary is circular and use the isotropic distribution function (1) with $p = 0$. In this case the evolution law of the binary separation distance is especially simple:

$$D(t) = r_a \exp(-t/T_{d.f.}), \quad 73$$

where r_a is the radius of the cusp (see Section 2), and the characteristic evolution time scale $T_{d.f.}$ can be easily obtained from the expressions given in Chandrasekhar 1960:

$$T_{d.f.} = \frac{1}{3\pi} q^{-1} \Lambda_c^{-1} P_a \approx 2 \cdot 10^4 \left(\frac{1 \cdot 10^{-2}}{q} \right) M_7^{-1/2} r_1^{3/2} \text{yr}, \quad 74$$

where $q = m/M$ is the binary mass ratio, $\Lambda_c \sim 15$ is the so-called Coulomb logarithmic factor, $r_1 = r_a/1\text{pc}$, and P_a is a typical period of the binary with separation distance $D \sim r_a$

$$P_a = 2\pi \sqrt{\frac{r_a^3}{GM}} \approx 3 \cdot 10^4 M_7^{-1/2} r_1^{3/2} \text{yr}. \quad 75$$

The evolution law (73) tells that the characteristic evolution time scale D/\dot{D} is independent of the distance D and is always approximately equal to $T_{d.f.}$.

Equation (73) has its limits of applicability. When the binary evolves to the radius $r_m = r_a q^{2/3}$ where the total mass of the stars inside the binary orbit is of order of the

secondary mass m the evolution is halted (Begelman, Blanford & Rees 1980).^{||} So we have $\tilde{D} > q^{2/3}$. On the other hand, the expression (73) is approximately valid only when the time $T_{d.f.}$ is larger than the binary orbital period

$$P_b = 2\pi\Omega_b^{-1} = P_a\tilde{D}^{3/2},$$

hence $\tilde{D} < (\frac{1}{3\pi q\Lambda_c})^{2/3}$. When the mass ratio of the binary is larger than a certain value q_{crit} both conditions are incompatible with each other and our simple description of the dynamical friction becomes qualitatively invalid. The value q_{crit} can be found by equating $T_{d.f.}$ and P_b at the radius r_m

$$q_{\text{crit}} = \frac{1}{\sqrt{3\pi\Lambda_c}} \sim 0.1, \quad 76$$

where we recall that $M_{st} = M\tilde{D}^{3/2}$ (equations (4) and (5) with $p = 0$) and use $\Lambda_c = 15$. When the mass ratio q is in the range: $\frac{1}{3\pi\Lambda_c} \sim 1 \cdot 10^{-2} < q < q_{\text{crit}} \sim 0.1$ equation (73) is approximately valid only for the dimensionless separation distance \tilde{D} smaller than

$$\tilde{D}_{\text{crit}} = \frac{1}{(3\pi\Lambda_c q)^{2/3}} = \frac{q_{\text{crit}}^{4/3}}{q^{2/3}} \approx 0.2 \left(\frac{q_{\text{crit}}}{q} \right)^{2/3}. \quad 77$$

6.3 The tidal disruption rate

The expression for the tidal disruption rate, \dot{M}_t is determined by the ratio of the characteristic time scale of the secular evolution given by equations (68) and (70) to the time scale of the dynamical friction $T_{d.f.}$. When this ratio is small, for a given value of the separation distance D almost all stars with semi-major axes of the order of D and sufficiently small values of the z component of angular momentum have a chance to be tidally disrupted. In this case \dot{M}_t can be expressed in terms of the time scale $T_{d.f.}$, the probabilities Pr_{tot} and $Pr_{\text{tot},1}$ given by equations (67) and (69), and the total mass of the stars within the sphere of radius D , $M_{st}(D)$. When $l_T \gg q$ we have

$$\dot{M}_t(D) \approx \frac{Pr_{\text{tot}} M_{st}(D)}{T_{d.f.}}, \quad 78$$

and in the opposite case $l_T \ll q$ we should use $Pr_{\text{tot},1}$ instead of Pr_{tot} in equation (78). When the time scales of the secular evolution are larger than $T_{d.f.}$ the bulk of the stars have no time to be tidally disrupted, and the tidal disruption rate is determined by equation (66):

$$\dot{M}_t(D) \approx \dot{P}r M_{st}(D). \quad 79$$

^{||} In fact, the evolution may proceed due to the effect of gas dynamic drag exerted on the binary by e.g., an accretion disc (Ivanov, Polnarev & Papaloizou 1999). We do not consider this possibility in the present paper.

As follows from equation (72) the size of the loss cone increases when the separation distance D decreases. That means that, in principal, the ratio $R = l_T/q$ is a function of scale. However, it is easy to see from equation (72) that when $q > 1 \cdot 10^{-2}$ we have $R < 1$ for the all scales of interest $r_m < D < r_a$, and when $q < 3 \cdot 10^{-3}$ we have $R > 1$ for the relevant scales. For simplicity we are going to consider separately two possible cases: 1) the case of a large mass ratio $q > 1 \cdot 10^{-2}$ and 2) the case of a small mass ratio $q < 3 \cdot 10^{-3}$.

In the case of the large mass ratio it can be easily shown that the time scale $T_{d,f}$ is always smaller than or of the order of the time scale $T_{*,1}$ given by equation (70). Accordingly, we can use equation (79) and obtain the explicit expression for \dot{M}_t with help of equations (66), (72) and (75):

$$\dot{M}_t \approx 4 \cdot 10^{-1} \left(\frac{q}{10^{-2}} \right)^{2/3} \mu^{-1/3} M_7^{5/3} r_1^{-2} \frac{M_\odot}{\text{yr}}, \quad (80)$$

where we use the radial variable $\mu = M_{st}(D)/m$ instead of D . It is obvious that the variable μ takes its values in the range $1 < \mu < q^{-1}$. \dot{M}_t decreases with increase of μ and therefore the innermost part of the cusp $\mu = 1$ gives the highest tidal disruption rate. Note, however, that this dependence is rather slow $\dot{M}_t \propto \mu^{-1/3}$.

In the case of the small mass ratio there is a scale μ_* where the secular time T_* given by equation (68) is equal to $T_{d,f}$:

$$\mu_* \approx \left(\frac{3 \cdot 10^{-3}}{q} \right)^2. \quad (81)$$

The tidal disruption rate is given by equation (80) for $\mu > \mu_*$. In the opposite case we use equation (78) with the result

$$\dot{M}_t \approx 2 \cdot 10^{-1} \left(\frac{q}{3 \cdot 10^{-3}} \right)^{5/3} \mu^{1/6} M_7^{5/3} r_1^{-2} \frac{M_\odot}{\text{yr}}. \quad (82)$$

The tidal disruption rate is maximal at $\mu = \mu_*$:

$$\dot{M}_{\text{max}} \approx 2 \cdot 10^{-1} \left(\frac{q}{3 \cdot 10^{-3}} \right)^{4/3} M_7^{5/3} r_1^{-2} \frac{M_\odot}{\text{yr}}. \quad (83)$$

Estimates of the tidal disruption rate in the astrophysical systems containing a single supermassive black hole give the value of the rate smaller than or of the order of $\dot{M}_* \sim 10^{-4} M_\odot/\text{yr}$ (e.g., Magorrian & Tremaine 1999, Syer & Ulmer 1999 and references therein). Equating \dot{M}_* to \dot{M}_{max} we can find the minimal mass ratio, q_{min} sufficient for the tidal disruption rate determined by the presence of the binary to surpass the standard value

$$q > q_{\text{min}} \approx 10^{-5} r_1^{3/2} M_7^{-5/4}. \quad (84)$$

There is another important limitation on our formalism determined by the relativistic effect of Einstein apsidal precession of the stellar orbits (Hopman & Alexander 2005). To

estimate the importance of this effect we use the standard expression for the change of the argument of pericentre due to this effect:

$$\delta\omega_{rel} = \frac{6\pi GM}{c^2 \epsilon_T^2 a},$$

where $\epsilon_T = l_T/\sqrt{\tilde{a}}$ is the value of the parameter ϵ associated with the 'tidal' angular momentum l_T . We calculate the corresponding precession rate $\dot{\omega}_{rel} = \delta\omega_{rel}/P_{orb}$, and compare it with the precession rate determined by the Kozai effect in the limit of high eccentricity: $\dot{\omega}_K \sim 5/(T_K \epsilon_T)$ (see equation 12). We find that the Einstein precession is not important provided that the mass ratio is sufficiently high:

$$q > q_{rel} \sim 1.5 \cdot 10^{-3} \frac{M_7^{5/6}}{\sqrt{\tilde{D}r_1}}, \quad 85$$

where we set $a = D/2$ for a 'typical' stellar orbit.'

Finally, let us estimate the duration of the phase of the enhanced tidal disruption rate due to the presence of the secondary. The corresponding time scale, T_T follows from equation (73)

$$T_T = \ln(r_a/r_m) T_{d.f.} = \frac{2}{3} \ln(q^{-1}) T_{d.f.} \quad 86$$

We also neglect the difference between D_{crit} (equation 77) and r_a which enters in the expression under the logarithm. Substituting equation (74) in (86) we find that T_T is rather short:

$$T_T = 6 \cdot 10^4 \left(1 + \frac{1}{4.6} \ln \frac{10^{-2}}{q} \right) M_7^{-1/2} r_1^{3/2} \text{yr}. \quad 87$$

7 CONCLUSIONS AND DISCUSSION

We have shown in this paper that the tidal disruption rate in a galactic cusp containing a circular black hole binary can be as large as $\sim 0.1\text{--}1M_\odot/\text{yr}$ for a cusp size of the order of 1pc. Cusps of this size have been observed in e.g. our own Galaxy and M32 (e.g. Kormendy & Gebhardt 2001 and references therein). In principle, the rate of gas supply to the centre of the galaxy is sufficient to power a quasar or a powerful AGN. However, the estimated duration of the stage of the enhanced tidal disruption rate $\sim 10^5\text{yr}$ seems to be much shorter than the expected life time of the central engine in quasars. Also, note that the tidal disruption rate sharply decrease with increase of the cusp size $r_a: \propto r_1^{-2}$, where $r_1 = r_a/1\text{pc}$. The observations suggest that the cusp size grows with mass of the central black hole with the typical sizes in the range 10 – 30pc for the masses of central black holes of the order of $10^7 - 10^8 M_\odot$

(e. g. Kormendy & Gebhardt 2001). So for an extended cusp of size $\sim 10\text{pc}$ we get rather moderate values of the tidal disruption rate of the order of $1 \cdot 10^{-3} - 1 \cdot 10^{-2} M_{\odot}/\text{yr}$.

The tidal disruption events in a system containing a supermassive black binary black hole could have observational consequences on its own. A single tidal disruption event could manifest itself as sharp rise of luminosity of a galactic centre on time scale $\sim 1\text{yr}$ (Gurzadian & Ozernoi 1981, Lacy et al 1982, Rees 1988, Komossa et al 2003 and references therein). The repeating luminosity flares in a particular galaxy could suggest that there is a binary black hole in the centre. On the other hand, one can expect the increased probability of the tidal disruption events in the supermassive binary black hole candidates (e.g., Sillanpaa et al 1988, Valtaoja et al 2000).

We assume that the stellar distribution has a pronounced density increase toward the centre. This assumption is well motivated from theoretical point of view and also has been confirmed by analysis of the distribution of stars inside our own Galaxy (e.g., Alexander 1999) and some other galaxies (e.g., Faber et al. 1997). However, after the intervention of the secondary black hole and coalescence with the primary, a large fraction of the stars is expelled from the centre, and the density increase is smeared out. This may explain rather shallow density profiles observed in the centers of bright galaxies (e.g., Faber et al. 1997). Thus, subsequent coalescence events of two black holes within the centre of the same galaxy would be accompanied by smaller numbers of tidally disrupted stars.

We have considered only the ‘inner problem’ where all stars going to the loss cone were assumed to be inside the binary orbit and showed that for the inner problem the bulk of the stars going to loss cone would have had a small value of the projection of the angular momentum on the axis perpendicular to the binary orbital plane before intervention of the secondary in the cusp. The mechanism responsible for the supply of the stars into the loss cone is analogous to the well known Kozai effect in celestial mechanics. However, the important effect of the oscillation of the angular momentum on the time scale of the order of the binary orbital period should also be taken into account in order to obtain the correct expression for the tidal disruption rate in a binary with a sufficiently large mass ratio. Also, we take into account the apsidal precession determined by gravitational potential of the stellar cluster itself and develop the analytical theory of secular evolution in the combined gravitational field of the binary and the stellar cluster. This theory might be useful in other astrophysical applications, such as e.g., the theory of dynamics of the triple stars (e.g.,

Kiseleva, Eggleton & Mikkola 1998 and references therein), and the theory of dynamics of extra-solar planets around the binary or a single star (e.g., Papaloizou & Terquem 2001).

The tidal disruption rate may be significantly enhanced if we take into account ‘the outer’ stars with semi-major axes larger than the half of the binary separation distance. The evolution of these stars in the binary gravitational field is mainly governed by two processes: the secular non-resonant interaction with the binary similar to the interaction discussed in our paper, and the effect of close encounters with the secondary which change the orbital elements of the star in a complicated chaotic way. Unfortunately, this problem looks very complicated for a thorough theoretical treatment and numerical calculations are very important in this case.

Our estimate of the rate of supply of the stars to the tidal loss cone relied upon the effect of the secular increase of the eccentricity. We have analysed this effect in an idealised situation where only the Keplerian gravitational field of the binary and corrections due to the stellar cluster have been taken into account and the binary has had a circular orbit with the fixed separation distance between the primary and the secondary. In a real astrophysical situation the binary could have a substantial eccentricity (e.g., Quinlan & Hernquist 1997, Aarseth 2003) and the orbital parameters of the binary are evolving with time due to the effect of dynamical friction. Therefore, a very important question arises: to what extent is the effect of the secular increase of the eccentricity of the stellar orbits sensitive to possible corrections due to non-zero eccentricity and to a change of the orbital elements of the binary? First we would like to point out that when the eccentricity of the binary is not very large the effects determined by the eccentricity seem to be rather insignificant for the inner problem considered above. Indeed, in the quadrupole approximation used in our analysis the gravitational field of the eccentric binary is formally equivalent to the gravitational field of the circular binary provided that we use the parameter of the binary orbit $p_B = a_B(1 - e_B^2)$ instead of the separation distance D in equation (14) defining the characteristic time-scale of the Kozai effect, T_K (e.g. Innanen, Zheng, Mikkola and Valtonen 1997). Of course, in the case of a highly eccentric binary the influence of the next order corrections in the small parameter a/D would be more prominent, but we expect that the qualitative character of the secular evolution would remain unchanged until the condition $a/D < 1$ holds for the stellar orbits of interest. When the quadrupole approximation is valid, a slow change of the orbital parameters of the binary also seems to be unimportant. In this case this time dependence enters the equations of the secular evolution (10–13) only through the time

dependence of the quantity $T_K(t)$ in front of the time derivatives. Introducing the new time variable $t_1 = \int dt/T_K$ we can eliminate this time dependence, and the secular evolution is the same in terms of the new time variable t_1 as it was in the case of the non-evolving binary orbital elements.

In this Paper we consider the black holes as point like sources of Newtonian gravity. However, as we discussed in the previous Section, the relativistic effect of Einstein apsidal precession (and, possibly, the effect of gravitomagnetic precession) could be important. A study of these effect could be a very interesting problem deserving a separate study.

In conclusion, we would like to point out that for a quantitative calculation of the tidal disruption rate our approach is perhaps too oversimplified, and a thorough numerical study is needed. However, our model can be used for the order of magnitude estimates discussed above. It can also be used for guidance on the choice of parameters in numerical studies.

ACKNOWLEDGEMENTS

It is a pleasure to thank J.C.B. Papaloizou for many important and fruitful discussions and comments. We also thank Clovis Hopman for useful remarks. The authors acknowledge support from PPARC through research grant PPA/G/02001/00486.

REFERENCES

- Aarseth, S. J., 2003, ApSS, 285, 367
 Alexander T., 1999, ApJ, 527, 835
 Bahcall J. N., Wolf R. A., 1976, ApJ, 209, 214
 Beloborodov, A. M., Illarionov, A. F., Ivanov, P. B., Polnarev, A. G., 1992, MNRAS, 259, 209
 Begelman, M. C., Blanford, R. D., Rees, M. J., 1980, Nature, 287, 307
 Chandrasekhar, S., 1960, Principles of Stellar Dynamics, New York: Dover
 Cohn H., Kulsrud R. M., 1978, ApJ, 226, 1087
 Faber, S. M., Tremaine, S., Ajhar, E. A., Byun, Y., Dressler, A., Gebhardt, K., Grillmair, G., Kormendy, J., Lauer, T., Richstone, D., 1997, AJ, 114, 1771
 Frank, J., Rees, M. J., MNRAS, 1976, 176, 633
 Gurzadian, M. J., Ozernoi, L. M., 1981, A&A, 95, 39
 Hills, J. G., 1975, Nature, 254, 295
 Hopman C, Alexander, T, unpublished
 Innanen, K. A., Zheng, J. Q., Mikkola, S., Valtonen, M. J., 1997, AJ, 113, 1915
 Ivanov, P. B., Chernyakova, M. A., Novikov, I. D., 2003, MNRAS, 338, 147
 Ivanov, P. P., Papaloizou, J. C. B., Polnarev, A. G., 1999, MNRAS, 307, 79
 Kiseleva, L. G., Eggleton, P. P., Mikkola, S., 1998, MNRAS, 300, 292
 Komberg, B. V., 1968, SvA, 11, 727

- Komossa, S., Halpern, J., Schartel, N., Hasinger, G., Santos-Lleo, M., Predehl, P., 2004, *ApJ*, 603L, 17
- Kormendy, J., Gebhardt, K., 2001, in: 20th Texas Symposium on relativistic astrophysics, AIP conference proceeding, 586, 363
- Kozai, Y., 1962, *AJ*, 67, 591
- Lacy, J. H., Townes, C. H., Hollenbach, D. J., 1982, *ApJ*, 292, 120
- Landau, L. D., Lifshitz, E. M., 1969, *Mechanics*, Oxford: Pergamon Press
- Lidov, M. L., 1961, in: *Iskusst. sputniky Zemly* 8, Acad. of Sci., USSR
- Lidov, M. L., 1962, *Planetary & Space Science*, 9, 719
- Lightman A. P., Shapiro S. L., 1977, *ApJ*, 211, 244
- Magorrian, J., Tremaine, S., 1999, *MNRAS*, 309, 447
- Merritt, D., Milosavljevic, 2004, astro-ph/0410364, to appear in *Living Reviews in Relativity*
- Papaloizou, J. C. B., Terquem, C., 2001, *MNRAS*, 325, 221
- Peebles, P. J. E., 1972, *ApJ*, 178, 371
- Polnarev, A. G., Rees, M. J., 1994, 283, 301
- Rees, M. J., *Nature*, 1988, 333, 523
- Quinlan, G. D., Hernquist, L., 1997, *NewA*, 2, 533
- Shapiro, S. L., Marchant, A. B., 1978, *ApJ*, 225, 603
- Sillanpaa, A., Haarala, S., Valtonen, M. J., Byrd, G. G., 1988, *ApJ*, 325, 628
- Spitzer L., 1987, *Dynamical evolution of globular clusters*, Princeton, NJ, Princeton University Press
- Syer, D., Ulmer, A., 1999, *MNRAS*, 306, 35
- Valtaoja, E., Terasanta, H., Tornikoski, M., Sillanpaa, A., Aller, M. F., Aller, H. D., Huges, P. A., 2000, *ApJ*, 531, 744
- Wang, J., Merritt, D., 2004, *ApJ*, 600, 149
- Young P., 1980, *ApJ*, 249, 1232

APPENDIX A: THE PRECESSION RATE

Here we derive expressions for the apsidal precession rate of a stellar orbit induced by the gravitational field of the stellar cusp. As follows from the discussion above the mass of the stars in the cusp M_{st} and accordingly the gravitational potential Φ_{st} depend on the radius r as a power of the radius

$$M_{st} = M \left(\frac{r}{r_a} \right)^{3/2-p}, \quad \Phi_{st} = \frac{GM}{(1/2-p)r_a} \left(\frac{r}{r_a} \right)^{1/2-p}, \quad A1$$

Assuming that $r \ll r_a$ we can consider Φ_{st} as a perturbation. In this case the change $\delta\omega$ of the angle ω per one orbital period is given by the expression (e.g., Landau, Lifshitz 1969)

$$\delta\omega = 2 \frac{d}{dL} \left(\frac{1}{L} \int_0^\pi d\phi (r^2 \Phi_{st}) \right), \quad A2$$

where the radius r is determined by the standard Keplerian relation

$$r = \frac{L^2}{GM(1 + e \cos(\phi))}. \quad A3$$

Substituting (A1) in (A2) and introducing the new variable $\epsilon = \sqrt{(1 - e^2)}$ instead of the eccentricity e we obtain

$$\delta\omega = \frac{2}{s-1} \left(\frac{a}{r_a} \right)^s \frac{d}{d\epsilon} (\epsilon^{2s+1} J), \quad A3$$

where $s = 3/2 - p$, a is the semi-major axis, we use $L = \sqrt{(GMa)\epsilon}$, and

$$J = \int_0^\pi \frac{d\phi}{(1 + e \cos \phi)^{s+1}}, \quad A4$$

When $s \neq n/2$ where n is an integer, the integral J can be expressed in terms of the Legendre function $P_s(x)$ as

$$J = \pi \epsilon^{-(s+1)} P_s(\epsilon^{-1}), \quad A5$$

and $P_s(x)$ is expressed itself in terms of the hyper-geometric function $F(\alpha; \beta; \gamma; x)$ as

$$P_s(x) = 2^s \sqrt{\pi} \frac{\Gamma(s+1/2)}{\Gamma(s+1)} x^s F((1-s)/2; -s/2; 1/2-s; 1/x^2) + \frac{\tan(s\pi)}{2^{s+1} \sqrt{\pi}} \frac{\Gamma(s+1)}{\Gamma(s+3/2)} x^{-s-1} F(s/2+1; (s+1)/2; s+3/2; 1/x^2), \quad A6$$

where $\Gamma(x)$ is the gamma function.

We are interested in $s = 3/2$ corresponding to $p = 0$. In this case the integral J can be expressed in terms of the complete elliptic integrals as

$$J = \frac{2}{3} \frac{\sqrt{(1+e)}}{\epsilon^4} \left(4\mathbf{E} \left(\sqrt{\frac{2e}{1+e}} \right) - (1-e)\mathbf{K} \left(\sqrt{\frac{2e}{1+e}} \right) \right). \quad A7$$

When eccentricity is small, the expressions are simplified significantly. In the leading order in the small parameter ϵ we obtain from equations (A3), (A5) and (A6)

$$\delta\omega = -K \left(\frac{a}{r_a} \right)^s \epsilon, \quad A8$$

where

$$K = \sqrt{\pi} \frac{2^{s+1}}{(2s-1)} \frac{\Gamma(s+1/2)}{\Gamma(s)}. \quad A9$$

Substituting $p = 3/2 - s$ in equation (A9) we obtain

$$K = 2^{3/2-p} \sqrt{\pi} \frac{\Gamma(1-p)}{\Gamma(3/2-p)}. \quad A10$$

In the case $p = 0$ ($s = 3/2$) we use equations (A3) and (A7) to obtain

$$\delta\omega = -4\sqrt{2} \left(\frac{a}{r_a} \right)^{3/2} \epsilon. \quad A11$$

Note that equation (A11) follows from equations (A8) and (A9) when $s = 3/2$.

APPENDIX B: EVOLUTION OF THE ANGULAR MOMENTUM

In the quadrupole approximation the rate of change of square of the angular momentum of a star on an elliptic orbit due to gravitational perturbation of a perturber of mass m is given by the expression:

$$\frac{d}{dt} L^2 = \frac{6Gm}{D^5} \{ (\vec{r} \cdot \vec{r}_p) (r^2 (\dot{\vec{r}} \cdot \vec{r}_p) - (\vec{r} \cdot \vec{r}_p) (\vec{r} \cdot \dot{\vec{r}})) \}, \quad B1$$

where D is the separation distance, \vec{r} is the radius vector of the star with coordinates $(x(t), y(t), z(t))$ and \vec{r}_p is the radius vector of the perturber with coordinates $(x_p(t) = D \cos(n), y_p = D \sin(n), 0)$, where $n = \Omega_p t + n_0$ and $\Omega_p = \sqrt{\frac{GM}{D^3}}$. In the expression in the braces in (A1) we can use the unperturbed values of $\vec{r}(t)$ and $\vec{r}_p(t)$. Since the orbit of the star is in general inclined with respect to the orbital plane of the perturber, it is convenient to introduce new coordinates associated with the orbital plane of the star where the radius vector of the star has two non-zero components: $(\tilde{x}(t), \tilde{y}(t), 0)$, and relate these coordinates to the coordinates $(x(t), y(t), z(t))$ with help of the Euler angles. We have

$$x = (\cos(\omega) \cos(\chi) - \sin(\omega) \sin(\chi) \cos(i))\tilde{x} - (\sin(\omega) \cos(\chi) + \cos(\omega) \sin(\chi) \cos(i))\tilde{y}, \quad B2$$

$$y = (\cos(\omega) \sin(\chi) + \sin(\omega) \cos(\chi) \cos(i))\tilde{x} - (\sin(\omega) \sin(\chi) - \cos(\omega) \cos(\chi) \cos(i))\tilde{y}, \quad B3$$

where i is the inclination, ω is the argument of pericentre and χ is the longitude of ascending node. $\tilde{x}(t)$ and $\tilde{y}(t)$ are given by the standard Keplerian expressions

$$\tilde{x}(t) = a(\cos(\xi) - e), \quad \tilde{y}(t) = a\epsilon \sin(\xi), \quad B4$$

where a is the semi-major axis, e is the eccentricity, $\epsilon = \sqrt{1 - e^2}$ and ξ is the eccentric anomaly. Substituting (B2-B4) into the expression in the braces in equation (B1) we have

$$A = -\epsilon D^2 a^4 B \dot{\xi}, \quad B5$$

where the variable A represents the expression in the braces and

$$B = (1 - e \cos(\xi))((\cos(\xi) - e)\epsilon \sin(\xi)(\alpha^2 - \beta^2) + ((\cos(\xi) - e)^2 - \epsilon^2 \sin^2(\xi))\alpha\beta), \quad B6$$

$$\alpha = \cos(\omega) \cos(\phi) + \sin(\omega) \sin(\phi) \cos(i), \quad \beta = \sin(\omega) \cos(\phi) - \cos(\omega) \sin(\phi) \cos(i), \quad B7$$

and $\phi = n - \chi$.

After averaging of (B5) over the orbital period of the star, P_{orb} , we obtain

$$\bar{A} = \frac{1}{P_{orb}} \int_0^{2\pi} d\xi A = -\frac{5}{2}(\alpha\beta)\epsilon e^2 D^2 a^4 \Omega, \quad B8$$

where $\Omega = \sqrt{\frac{GM}{a^3}}$. Substituting (B8) into (B1) and taking into account the standard relation $L = \epsilon \sqrt{GMa}$, we obtain:

$$\frac{d}{dt}L = -\frac{15}{2}(\alpha\beta)e^2 \left(\frac{a}{D}\right)^3 \frac{Gm}{a}, \quad B9$$

where

$$\alpha\beta = -\frac{1}{2} \sin(2\phi) \cos(i) \cos(2\omega) + \frac{1}{4} \sin(2\omega)(\sin^2(i) + \cos(2\phi)(1 + \cos^2(i))). \quad B10$$

After averaging over the binary period equation (B9) must agree with equation (10). Taking into account that the averaged value of $\alpha\beta$ is equal to $\frac{1}{4}\sin(2\omega)\sin^2(i)$ and using $e = \sqrt{1 - \frac{L^2}{GMa}}$, we obtain:

$$\frac{d}{dt}e = \frac{15}{8}q\epsilon e \sin(2\omega) \sin^2(i) \left(\frac{a}{D}\right)^3 \Omega, \quad B11$$

where $q = m/M$. It is easy to see that equation (B11) is identical to equation (10).

Now let us estimate the amplitude of oscillations of the angular momentum ΔL on time scale comparable to the orbital period of the perturber. Neglecting for a moment these oscillations and assuming that the eccentricity of the star due to evolution of the orbital elements on the ‘slow’ Kozai time scale is close to its maximal value, and accordingly, the angular momentum is close to its minimal value L_{\min} , it follows from the discussion above that the inclination i_{\min} is minimal and $\omega \approx \pm\frac{\pi}{2}$. Therefore, we have $\alpha\beta \approx -\frac{1}{2}\cos(i_{\min})\sin(2\phi)$ from (A10), and equation (B9) takes the form:

$$\frac{d}{dt}L \approx -\frac{15}{4}\cos(i_{\min}) \left(\frac{a}{D}\right)^3 \left(\frac{Gm}{a}\right) \sin(2\phi). \quad B12$$

Integrating (B12) we obtain:

$$L \approx L_{\min} + \Delta L \cos(2\phi), \quad B13$$

where

$$\Delta L = \frac{15}{8}\cos(i_{\min})q \left(\frac{a}{D}\right)^2 \sqrt{GMD}. \quad B14$$

This paper has been produced using the Royal Astronomical Society/Blackwell Science L^AT_EX style file.